

APJHAD

Academic Platform

Journal of Natural Hazards

And Disaster Management

Volume: 5
Issue: 1
Year: 2024

Academic Platform Journal of Natural Hazards and Disaster Management (APJHAD)

Volume 5 Issue 1, June 2024

Contents

Research Articles

Title	Authors	Pages	
An Innovative Retrofitting Technique of an Industrial Prefabricated Building Without Evacuation	Suat Yıldırım, Yüksel Ilkay Tonguc	1	29
Cloudbursts Strike over Foothills Himalaya of Uttarakhand, India: A Case Study from Maldeota, Dehradun District	Sushil Khanduri	30	45

Academic Platform Journal of Natural Hazards and Disaster Management (APJHAD) Editorial Boards

Editor-in-Chief

Prof. Dr. Naci ÇAĞLAR, Bursa Technical University, Türkiye

Associate Editors

Asst. Prof. Dr. Abdulkadir ÖZDEN, Sakarya University of Applied Sciences, Türkiye

Editors

Assoc. Prof. Dr. A. Can ZÜLFİKAR, Gebze Technical University, Türkiye

Asst. Prof. Dr. Abdelrahman KHALIFA, Al-Azhar University, Egypt

Dr. Ana M. PETROVIC, Geographical Institute "Jovan Cvijić" Sasa, Serbia

Dr. Ana Mafalda MATOS, University of Porto, Portugal

Asst. Prof. Dr. Andrea MIANO, University of Naples Federico II, Italy

Asst. Prof. Dr. Beytullah EREN, Sakarya University, Türkiye

Asst. Prof. Dr. Cengiz ZABCI, Istanbul Technical University, Türkiye

Assoc. Prof. Dr. Ertan BOL, Sakarya University, Türkiye

Esequiel MESQUITA, Universidade Federal Do Ceará, Brazil

Prof. Dr. Fatih ALTUN, Erciyes University, Türkiye

Assoc. Prof. Dr. Fatih KIRIŞIK, Kütahya Dumlupınar University, Türkiye

Assoc. Prof. Gürsel SUNAL, Istanbul Technical University, Türkiye

Assoc. Prof. Dr. Hamide TEKELİ KABAŞ, Süleyman Demirel University, Türkiye

Prof. Dr. Hasan ARMAN, United Arab Emirates University, United Arab Emirates

Asst. Prof. Dr. İlyas SARIBAŞ, Adana Alparslan Türkeş Science and Technology University, Türkiye

Assoc. Prof. Dr. Junwon SEO, South Dakota State University, United States

Asst. Prof. Dr. Matteo PICOZZI, Università degli Studi di Napoli Federico II, Italy

Prof. Dr. Mehmet İNEL, Pamukkale University, Türkiye

Prof. Dr. Mehmet İshak YÜCE, Gaziantep University, Türkiye

Prof. Dr. Murat Emre KARTAL, İzmir Democracy University, Türkiye

Prof. Dr. Murat PALA, Adıyaman University, Türkiye

Assoc. Prof. Dr. Neritan SHKODRANI, Polytechnic University of Tirana, Albania

Dr. Nikolaos THEODOULIDIS, Institute of Engineering Seismology and Earthquake Engineering Research and Technical Institute, Greece

Prof. Dr. Osamu TAKAHASHI, Tokyo University of Science, Japan

Assoc. Prof. Dr. Ramazan CANSOY, Karabük University, Türkiye

Dr. Tuba TATAR, Sakarya University, Türkiye

Assoc. Prof. Dr. Vladimir CVETKOVIĆ, University of Belgrade, Serbia

Assoc. Prof. Dr. Yasmeeen Taleb OBAIDAT, Jordan University of Science And Technology, Jordan

English Language Editor

Asst. Prof. Dr. İsmail Gürler, Sakarya University of Applied Sciences, Türkiye

Technical Editor

Assoc. Prof. Dr. Caner ERDEN, Sakarya University of Applied Sciences, Türkiye

Res. Assist. Hasanburak YÜCEL, Ankara Yıldırım Beyazıt University, Türkiye

Res. Assist. Yusuf Bahçacı, Karabük University, Türkiye





Research Article

Academic Platform Journal of Natural Hazards and Disaster Management
5(1), 2024: 1-29, 2024 DOI: 10.52114/apjhad.1328346



An Innovative Retrofitting Technique of an Industrial Prefabricated Building without Evacuation

Suat Yıldırım^{1,2*} , Yüksel İlkey Tonguç² 

¹YLD Yildirim Muhendislik A. S., Engineering and Consultancy, Türkiye

²Promer Engineering and Consultancy, Türkiye

Received: / Accepted: 16-July-2023/ 02-May-2024

Abstract

This paper presents a seismic retrofit of an industrial-type precast reinforced concrete building structure using friction dampers. The project consisted of retrofitting two precast reinforced concrete buildings, one of which will be presented in this paper. Precast concrete is one of the industrial structures' most preferred construction methods due to its low cost, fast construction, and availability in rural areas. Unfortunately, most structures constructed before “Specification for Buildings to be Built in Seismic Zones (TBEC-2018) [1]” are not sufficiently engineered and are expected to perform poorly when exposed to a significant seismic event. The general characteristic of precast reinforced concrete buildings built before TBEC-2018 is their relatively high concrete quality (compared to cast-in-place reinforced concrete buildings) and better reinforcement workmanship. But they have some characteristic weaknesses as well. Weak beam-column connections, high drift ratios due to heavy beams, instability problems, and lack of frame behavior can be considered primary weaknesses. General classical retrofitting techniques include increasing beam/column sections or adding new reinforced concrete or steel members to the system or FRP (fiber-reinforced polymer) wrapping. Mostly classical retrofitting needs additional foundations. All these techniques require a long construction period, causing evacuation and stopping building usage. Because stopping the production cost can be tolerated by the owners, a retrofitting approach that can be assembled during the normal function of the industrial structures is required. As a result of this requirement, friction dampers are selected as the supplemental energy dissipation device. ASCE 41-17 [2] and ASCE 7-16 [3] are employed for the damper design and damping calculations. Before the damper study, some instability and weak connection problems are solved by traditional strengthening measures. The most effective damper configuration and capacities are selected after an iterative trial-and-error linear study using the simplified methods developed by PROMER. Nonlinear push-over analyses are conducted after linear pre-studies. Finally, a nonlinear time-history analysis is performed for confirmation of the results. It is shown that the proposed retrofit scheme satisfies the desired performance goals for both DD-1 [1] and DD-2 [1] events. Overall, it is considered that the proposed retrofit scheme with dampers provides the optimal solution for the project stakeholders from a performance, design, constructability, and economic point of view. Some application visuals will be presented, and methods will be explained in detail in the article. The friction damper behavior is based on the rotational friction hinge concept. The dampers increase building damping, causing a decrease in earthquake demand. As a result, dampers provide passive energy dissipation and protect buildings from structural and nonstructural damage during moderate and severe earthquakes.

Key words: Retrofitting, Friction dampers, Precast structures, Earthquake protection, Passive control

*Corresponding Author e-mail: suat@yildirimeng.com.tr

1. Introduction

Earthquakes have posed the most significant threat to life and caused the highest economic losses in Turkey. Since 1900, 76 earthquakes have resulted in approximately 90.000 fatalities, impacting a total population of 7 million and causing direct losses exceeding US\$25 billion. Notably, about half of these fatalities occurred due to two major earthquakes on the North Anatolian Fault in 1939 and 1999. The 1999 Marmara earthquakes, affecting ten cities (including six in the Marmara Region), resulted in a death toll exceeding 18,000 and a direct economic impact estimated at US\$5 billion (2.5% of GNP).

Prefabricated buildings, particularly those constructed before the implementation of the 2018 Turkish Earthquake Code (TBEC-2018), exhibit significant vulnerabilities in earthquake resistance. Numerous studies have identified and documented these weaknesses [4, 5].

Prefabricated structures are often the preferred choice for industrial buildings in Turkey. Research indicates that 75-85% of industrial buildings in Turkey's industrial regions are prefabricated [6, 7]. Moreover, research has shown that 80% of prefabricated buildings in the Adapazarı Organized Industrial Zone suffered partial or total damage during the 1999 Marmara earthquake [4, 5].

One of the main challenges in retrofitting industrial buildings is the need to cease operations during construction, which can be costly and disruptive. This study presents a novel approach to retrofitting a reinforced concrete prefabricated building using friction-type energy dissipating devices (FDD) without interrupting operations.

The retrofitting design process involves three main stages:

- 1- **Data Collection:** This stage includes material and soil testing, assessment analysis, and building design. Geometrical data is collected from the building, architectural and structural drawings are prepared, and material tests are conducted to determine concrete quality. The existing concrete compressive strength is determined as 26,3 MPa as per TBEC-2018. Reinforcement is determined as StIII using destructive and non-destructive methods. The target performance level for the building is established as "limited damage" under DD-2 earthquake conditions.
- 2- **Assessment Analysis:** This stage utilizes the fixed single-mode pushover nonlinear static analysis method via Etabs ver. 18 [8], as described in TBEC-2018 sections 5 and 15.
- 3- **Retrofitting Analysis and Design:** Since FDD is preferred for retrofitting and TBEC-2018 does not provide design procedures for structures containing FDD, ASCE 41-17 and ASCE 7-16 are used as reference standards. The fixed single nonlinear static pushover method is employed for retrofitting analysis of the building with dampers. Additionally, nonlinear dynamic time history analyses are performed for two selected earthquakes, fulfilling the reviewer's request even though not explicitly required by codes. Furthermore, the design addresses stability issues identified in the building beyond solely addressing performance concerns.

This study demonstrates the successful implementation of FDD for retrofitting a prefabricated industrial building without interrupting operations. This approach offers a promising solution for enhancing the earthquake resistance of existing prefabricated structures while minimizing downtime and associated costs.

2. Building Information

The building consists of two adjacent blocks: B1 (3-storey precast reinforced concrete) and B2 (4-storey cast-in-place monolithic). Although both blocks were retrofitted using friction dampers, this paper focuses solely on B1. Table 1 summarizes some of their key properties.

Table 1. General building properties

Storey #	B1 block 3 storey B2 block 4 storey	B1 BLOCK				
Concrete Compressive Strength:	B1 block 26,3 Mpa B2 block 15,4 Mpa	Story Name	Story Number	Height (m)	Area (m ²)	
Area	B1 block 9.481,40 m ² B2 block 1.040,20 m ²	Ground Floor	1	5,6	6320,75	
Rebar type	ST420	1. Floor	2	2,6-3,6	1580,31	
Foundation Type	Single footing	2. Floor	3	3,9-4,2	1580,31	

The prefabricated reinforced concrete structure, designated as B1, serves as a warehouse for a food production factory. While the main building consists of a single story, one section of the building incorporates two administrative mezzanine floors (Figure 2). The total building dimensions are 90 meters x 77 meters with 4 x 22,5 meter and 10 x 7,7 meter axes in the long and short directions, respectively (Figure 1). The overall building height is 12,0 meters, with two mezzanine administrative floors positioned at levels of 5,5 meters and 8,2 meters within the designated axis (Figure 2).

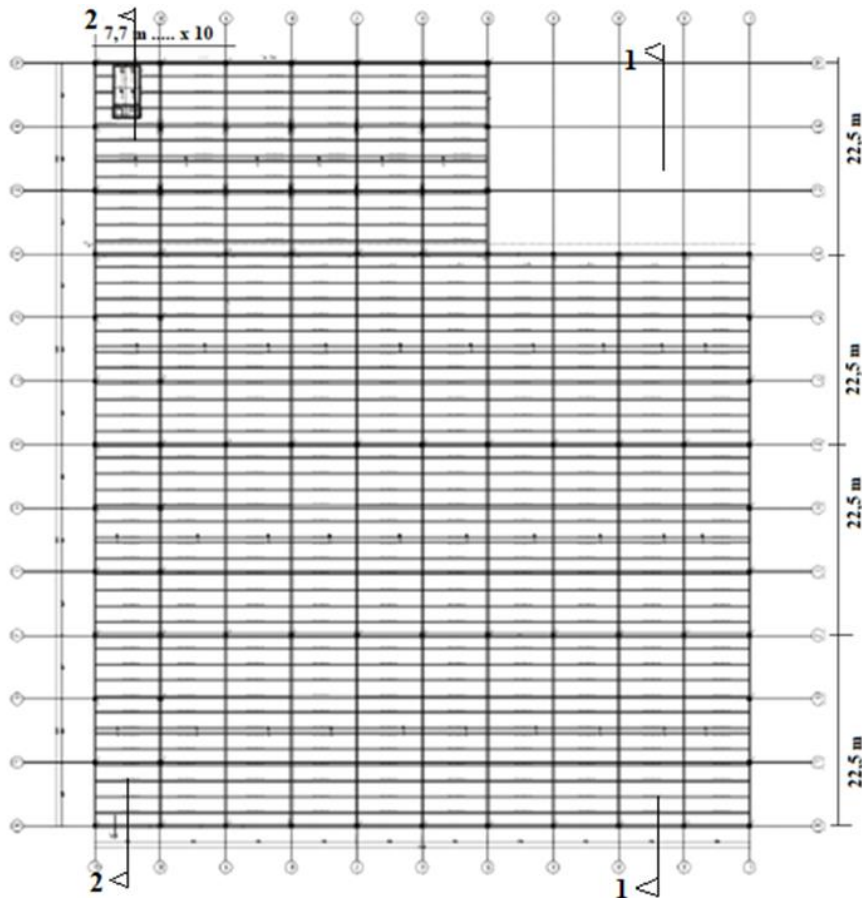


Figure 1. Plan view of the building

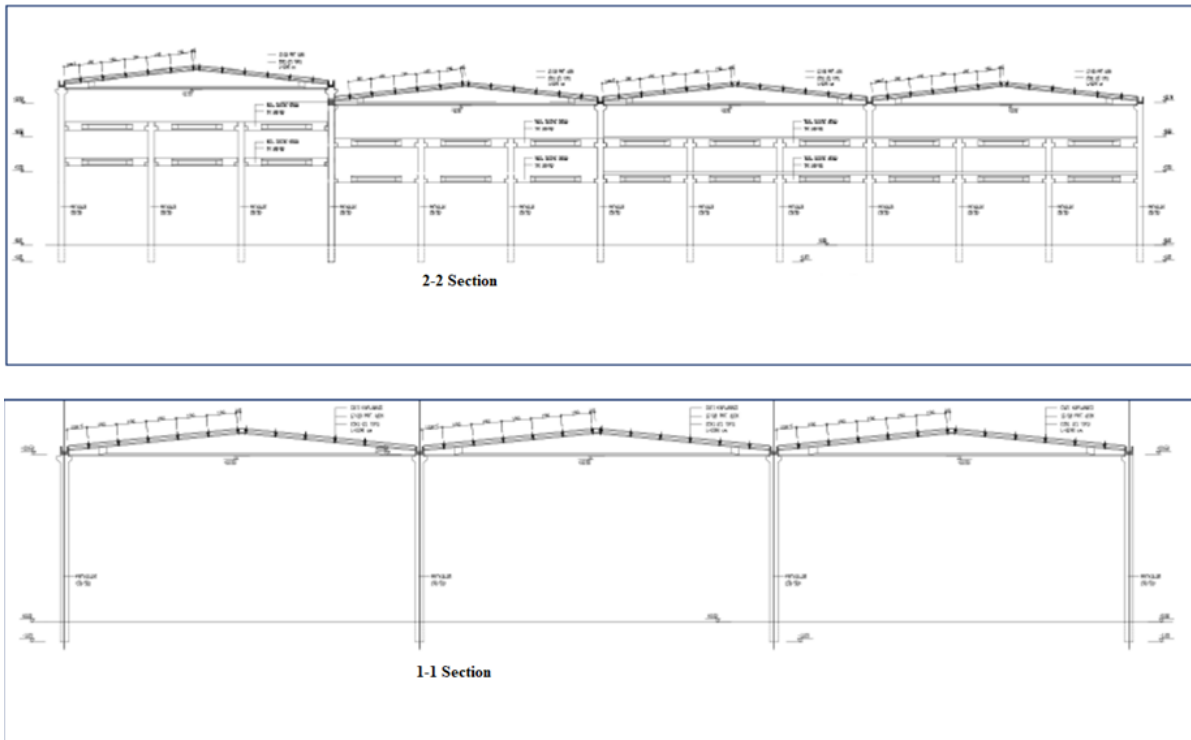


Figure 2. Section views of the building

Foundation System determination is based on construction project drawings provided by the client and confirmed by the excavation of two foundation test pits (Figure 3), the building utilizes a single-footing foundation system. The individual footings measure 360 centimeters by 360 centimeters with a height of 70 centimeters.



Figure 3. Foundation test pit excavation

2.1 Material Tests

While the client provided construction drawings for the prefabricated reinforced concrete (R/C) building, the lack of mechanical strength tests for the rebars necessitated a limited knowledge level approach for data collection. Therefore, a 0,75 capacity decrease was applied to member capacities according to TBEC-2018.

To assess concrete quality, 17 core samples were extracted from selected columns (Figure 4). The compressive strength was calculated based on TBEC-2018 and determined to be 26,3 MPa for the B1 block. Additionally, reinforcement type, orientation, diameter, and corrosion levels were determined for 11 columns using a stripping-destructive method (Figure 5).



Figure 4. a) b) Concrete core sampling



Figure 5. Reinforcement detection by stripping

Furthermore, Ferro-scan technology was employed on 19 vertical members to accurately determine the number and orientation of the reinforcing bars (Figure 6).

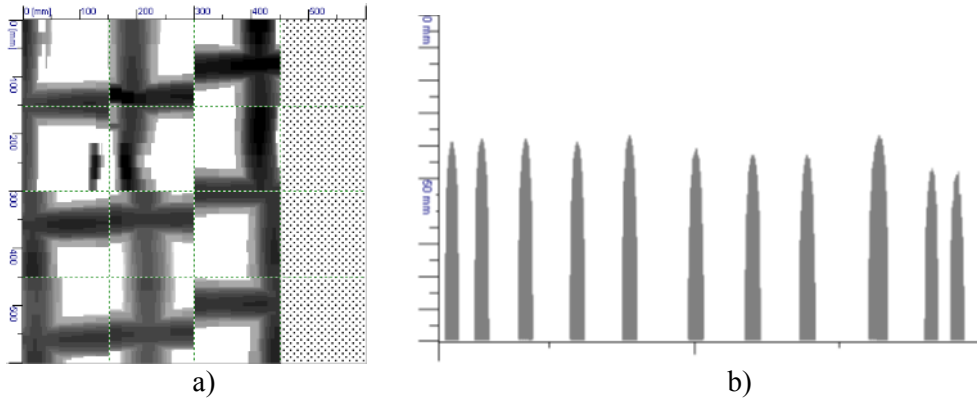


Figure 6. a) 60cmx60cm scan view from a column b) Vertical scan view of a column starting from the bottom. (1,6m-1,8m length)

The determined reinforcement layout and details are presented in Figure 7 and Table 2. No corrosion and foundation settlement are detected in the structure.

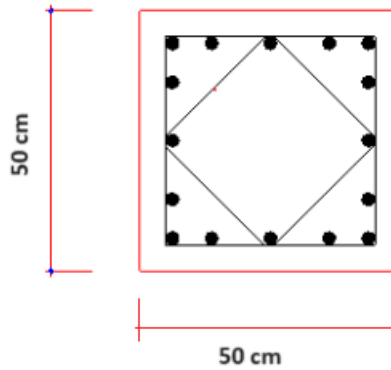


Figure 7. Determined reinforcement layout in a 50cmx50cm column

Table 2. Determined reinforcement details for column, shear wall, and beams

Member Type	Dimension (cmxcm)	Reinforcement Type	Vertical Reinforcement Diameter (pcs/mm)	Lateral Reinforcement Type	Lateral Reinforcement Span	Confinement
Column	50x50	StIII	16 pcs 20mm dia.	StIII	8 mm dia/ 20cm - 10cm interval	No
Shear Wall	25	StIII	14mm dia / 18cm interval	StIII	12mm dia/ 20cm interval	No
Beam		StIII		StIII	8mm dia/ 20cm interval	No

3. Modeling and Assessment Analysis

3.1. Assessment Conditions

3.1.1 Structural Performance Criteria

The Turkish Earthquake Code (TBEC-2018) does not include specific analysis criteria for structures incorporating energy dissipation devices. However, it allows the use of recognized international codes for subjects not addressed within its regulations. Therefore, while earthquake and performance damage levels are based on TBEC-2018, damping analysis will be conducted according to ASCE 41-17 and ASCE 7-16.

TBEC-2018 defines three primary structural performance levels:

- Limited Damage Level (SH): Minimal damage to structural elements.
- Controlled Damage Level (KH): Repairable but significant damage to structural elements.
- Collapse Prevention (GÖ): Avoidance of total collapse, but potentially severe damage.

These performance levels correspond to varying degrees of damage in lateral force-resisting systems. Additionally, the design process considers four earthquake ground motion levels that are DD-1, DD-2, DD-3[1], DD-4 [1].

As a production facility, the minimum acceptable performance level for the building is Controlled Damage Level (KH) under the DD-2 earthquake level, according to TBEC-2018. However, this implies substantial, repairable damage. The client, therefore, requested the Limited Damage Level (SH) as the target performance objective.

TBEC-2018 provides descriptions of expected damage under each performance level:

- KH (Operational Usage): No or negligible damage to both structural and non-structural systems.
- SH (Limited Damage): Acceptable probability of limited structural damage. Basic vertical and lateral-force resisting systems retain almost all pre-earthquake strength and stiffness.

ASCE 7-16 further clarifies the state of non-structural components at the Immediate Occupancy (IO) performance level:

- Minor cracking of facades, partitions, and ceilings.
- Equipment and contents generally secure but may not operate due to mechanical failure or lack of utilities.

3.1.2 Building Assessment Parameters

Table 3 summarizes the parameters utilized in the assessment. Earthquake spectrum parameters were obtained from the interactive earthquake map provided by AFAD (Turkish Disaster and Emergency Management Presidency) using local soil properties and coordinates.

Table 3. Building assessment and loading parameters

Building Importance Factor (I)	1	Roof LL: 1,5 kN/m ²	Corridor and Office rooms LL: 3,5 kN/m ²
EQ Load Reduction Factor (R)	1	Mezzanine LL : 2,0 kN/m ²	Snow Load: 0,75 kN/m ²
Soil Type	ZB	Brick Wall weight : 3,2 kN/m ²	
Cracked Section Rigidity Factor	0,4	Wind Load is as per TS EN 1991-I-3 (Eurocode 1)	
Soil Bearing Capacity (kPa)	400		
DD-1 Spectrum Parameters (AFAD)		DD-2 Spectrum Parameters (AFAD)	DD-3 Spectrum Parameters (AFAD)
$S_S = 1,326$ $S_1 = 0,367$ $PGA = 0,540$ $PGV = 33.247$		$S_S = 0,737$ $S_1 = 0,213$ $PGA = 0,308$ $PGV = 19.186$	$S_S = 0,286$ $S_1 = 0,087$ $PGA = 0,122$ $PGV = 8.087$
$S_{DS} = S_S \times FS = 1,326 \times 0,900 = 1,193$		$S_{DS} = S_S \times FS = 0,737 \times 0,900 = 0,663$	$S_{DS} = S_S \times FS = 0,286 \times 0,900 = 0,257$
$S_{D1} = S_1 \times F1 = 0,367 \times 0,800 = 0,294$		$S_{D1} = S_1 \times F1 = 0,213 \times 0,800 = 0,170$	$S_{D1} = S_1 \times F1 = 0,087 \times 0,800 = 0,070$

LL: Live Load

S_S : Short period spectral acceleration multiplier (unitless)

S_1 : Spectral acceleration multiplier for 1 sec. Period (unitless)

S_{DS} : Short period design spectral acceleration multiplier (unitless)

S_{D1} : Spectral design acceleration multiplier for 1 sec. Period (unitless)

PGA: Peak Ground Acceleration

PGV: Peak Ground Velocity

3.2 Modeling

A three-dimensional (3D) model of the building was constructed using ETABS software (Figure 11). Live and dead loads acting on the roof were calculated and distributed appropriately to the supporting beams. On the mezzanine floors, live and dead loads were directly assigned to the respective slabs.

For the concrete behavior, the Mander model was utilized to capture both confined and unconfined conditions (Figure 10). For the steel behavior, the Kinematic model was chosen to accurately represent its nonlinear response.

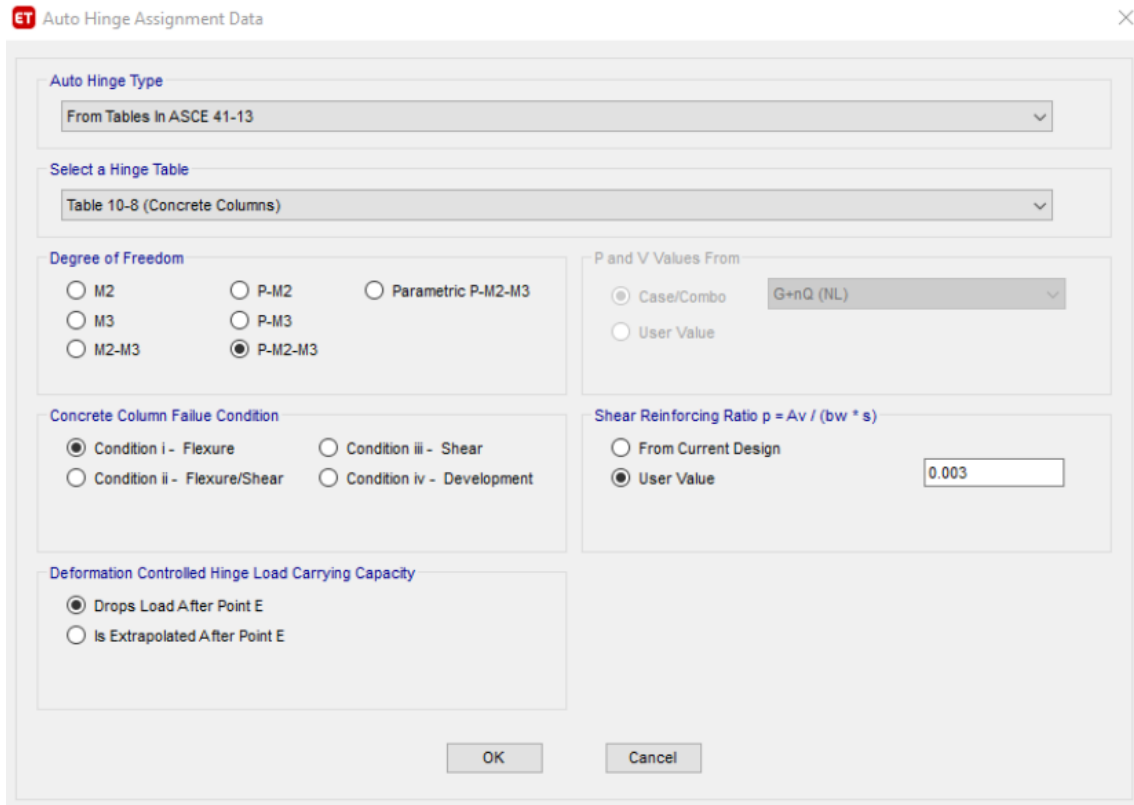


Figure 8. P-M2-M3 auto hinge modeling for columns

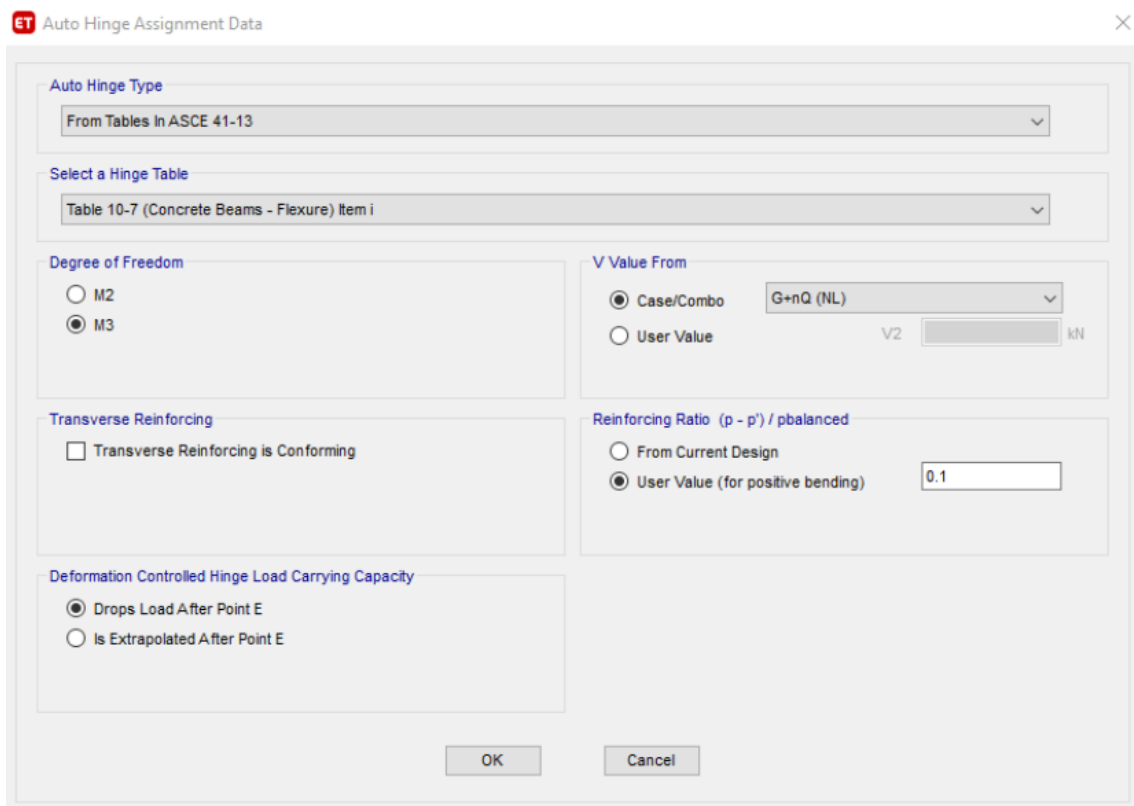


Figure 9. M3 auto hinge modeling for beams

An Innovative Retrofitting Technique of an Industrial Prefabricated Building without Evacuation

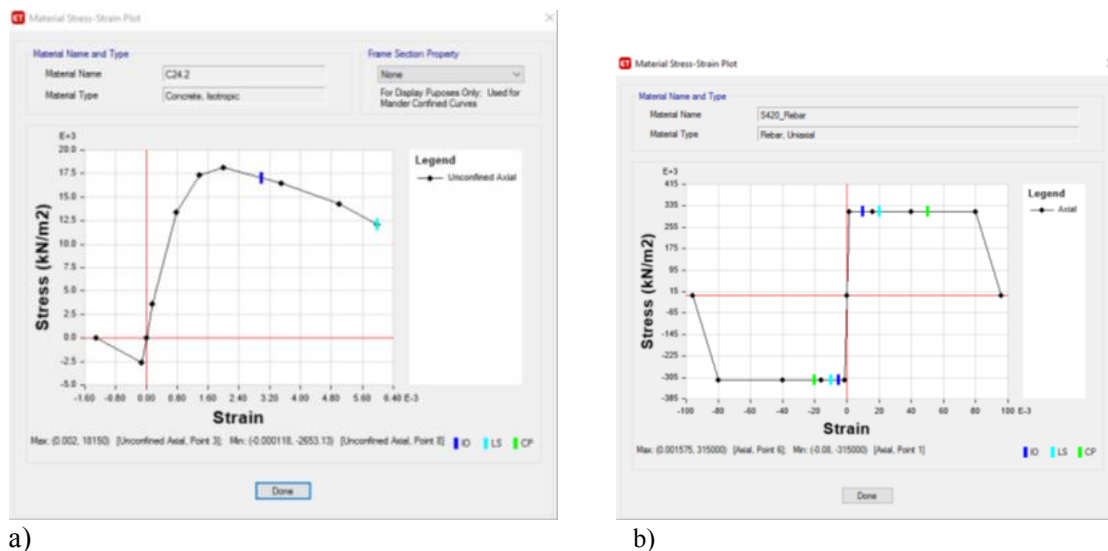


Figure 10. Nonlinear material model of a) concrete b) steel

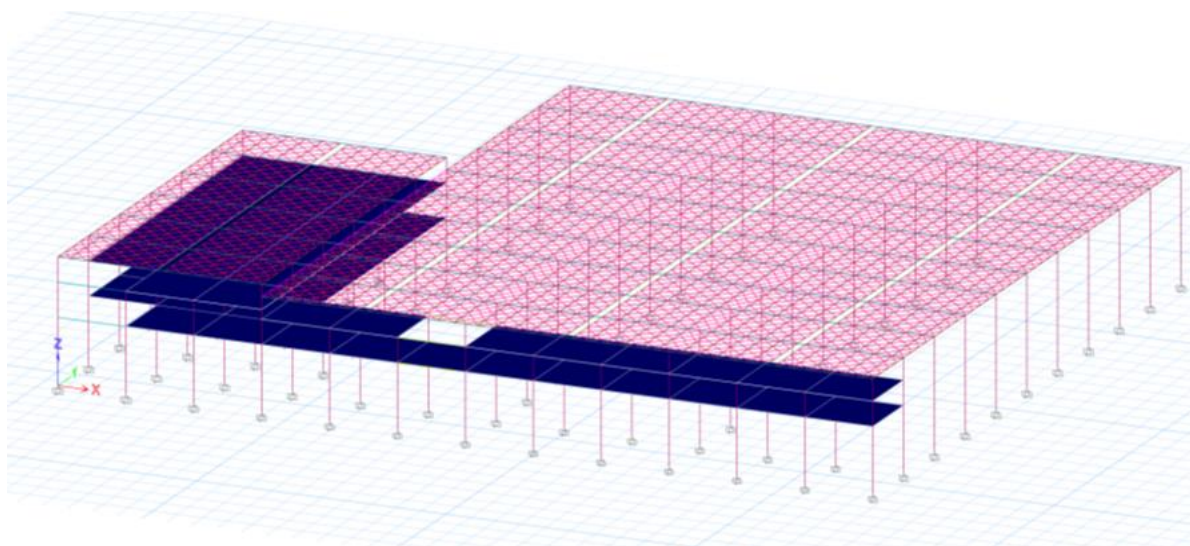
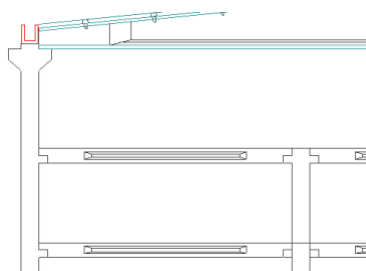


Figure 11. 3-D Etabs model perspective view

Both columns and beams were modeled as frame members within the Etabs software. Non-moment transferring beam column connections were represented as M3 releases and Nonlinear behavior was incorporated using designated hinge elements. Prefabricated beams with non-moment transferring connections accepted to be linear where as, columns utilized P-M2-M3 nonlinear hinges for comprehensive representation of axial and flexural behavior (Figures 8, 9, and 12).



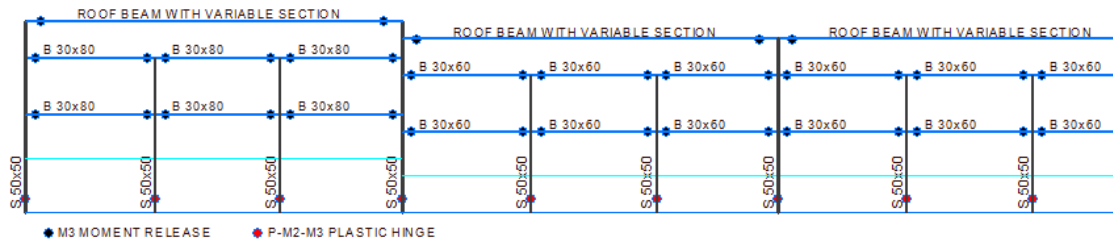


Figure 12. Nonlinear hinge definition for columns and beams

Modeling Roof Panel Rigidity:

The roof panel rigidity is modeled as per the definition outlined in TBEC-2018 Annex 8B (Figure 13). Rigidity is defined by the cross members connecting roof girder members at the panel level.

As specified in TBEC-2018, the rigidity of these cross members is calculated as $(EA)_e \approx 400.000 \text{ kN}$.

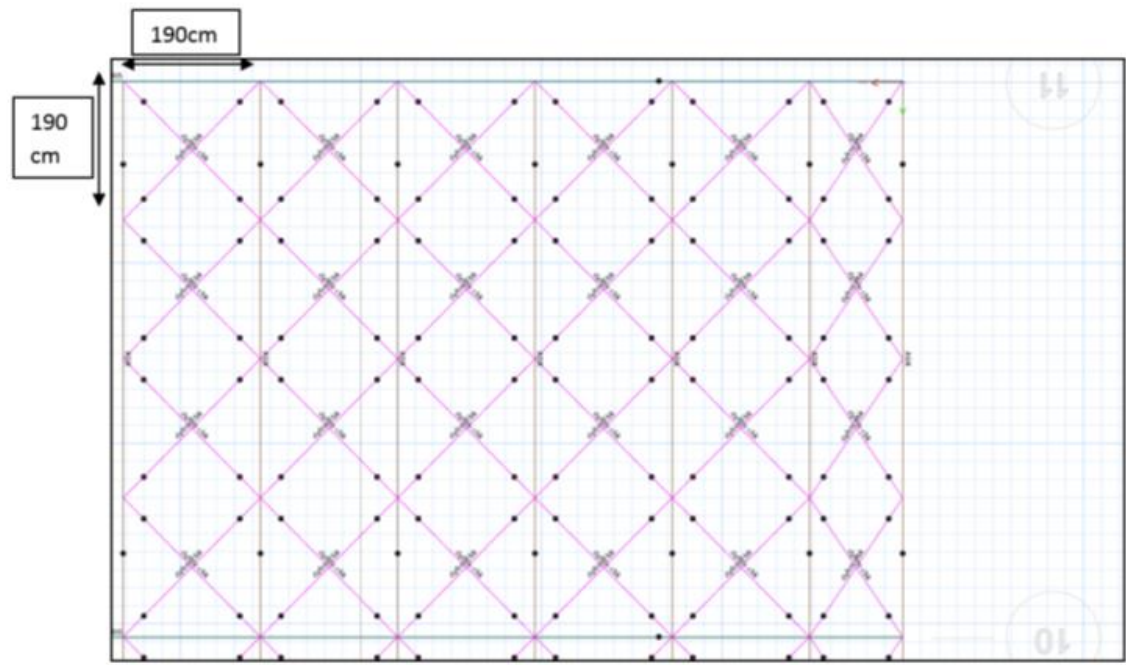


Figure 13. Roof rigidity modeling as per TBEC-2018 attachment 8B

3.3 Assessment Analysis of Existing Building

3.3.1 Linear Dynamic Analysis

A linear dynamic analysis (modal analysis) was conducted for the existing building conditions. The resulting modal participating mass ratios are presented in Table 4. The first mode corresponds to motion in the X-direction with a period of 3,686 seconds and a modal participation ratio of 0,891. The second mode represents Y-direction motion with a period of 3,33 seconds and a modal participation ratio of 0,7789.

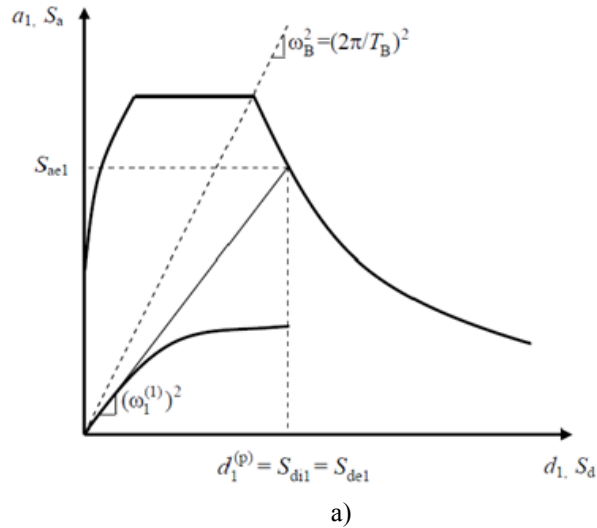
Since the effective modal mass participations exceed 0,70 and the story torsion remains within the acceptable limit (1,4), a nonlinear fixed first-mode pushover analysis will be employed as per TBEC 2018.

Table 4. Modal participating mass ratios

Case	Mode	Period (sec)	UX	UY
Modal	1	3,686	0,891	0,0003
Modal	2	3,33	0,0005	0,7789
Modal	3	3,031	3,81E-06	0,1275
Modal	4	2,49	0,0083	0,0002
Modal	5	1,544	0,0016	0,0006
Modal	6	1,247	0,0032	0,0019
Modal	7	1,116	0,0007	0,0072
Modal	8	1,077	0,0005	0,0035
Modal	9	0,99	0,0006	0,0001
Modal	10	0,94	0,0001	0,02
Modal	11	0,931	6,18E-07	0,0021
Modal	12	0,822	0,0051	0,0036

3.3.2 Performance Analysis Using Nonlinear Fixed First Mode Pushover

The procedure for fixed first-mode pushover analysis outlined in TBEC-2018 was followed (Figure 14). Pushover analyses were performed for both the X and Y directions separately. Each analysis was continued until the top floor displacement reached 4% of the building height, generating corresponding capacity curves (Figures 15 and 16).



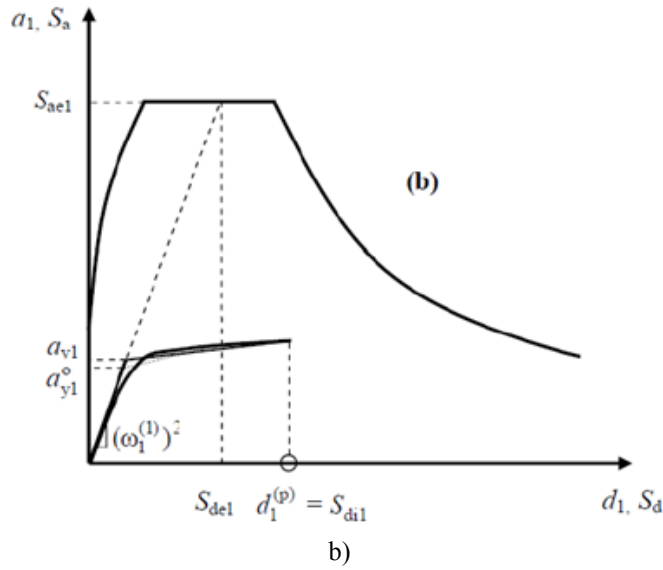


Figure 14. Target displacement calculation as per TBEC-2018 a) $T_1 > T_B$ b) $T_1 < T_B$

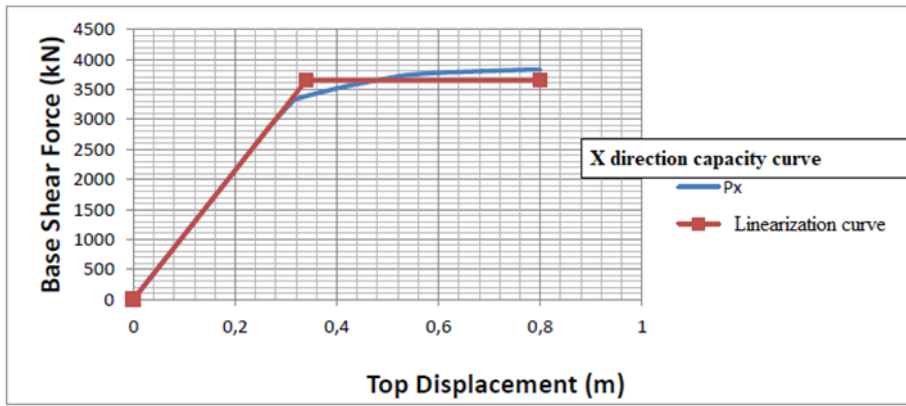


Figure 15. X direction capacity curve

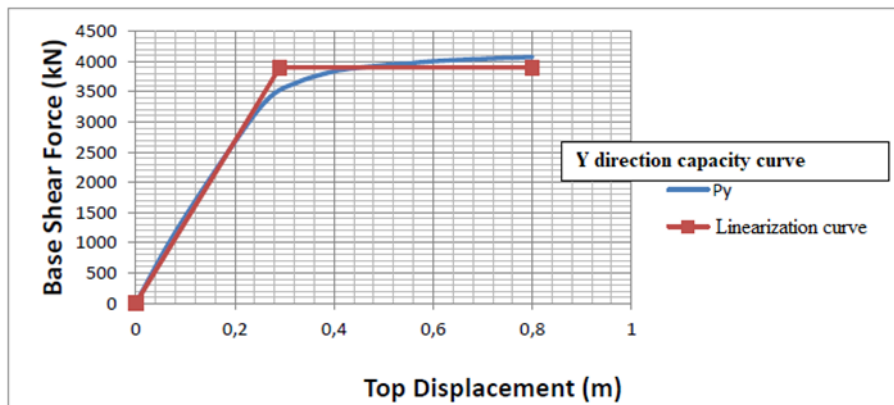


Figure 16. Y direction capacity curve

The target displacement was calculated following the procedure described in TBEC-2018 (Figure 14). The calculated target displacement and related parameters are presented in Table 5. Detailed calculations are not included in this paper as they conform to a standard procedure.

Table 5. Target displacement calculation for x and y direction

Tx (s)	Sae(T)/g	Sae(T)	Sde(m)	ay1	Ry1	CR1	Sdi1	Target Disp. (m) UxN1
3,686	0,04612	0,45244	0,15571	0,80325	0,56326	1	0,15571	0,155708931

Ty (s)	Sae(T)/g	Sae(T)	Sde(m)	ay1	Ry1	CR1	Sdi1	Target Disp. (m) UyN1
3,333	0,05101	0,50036	0,1408	0,85827	0,58299	1	0,1408	0,140797034

Tx (s): Natural vibration period

Sae(T): Lateral elastic design spectral acceleration

Sde(m): Lateral elastic design spectral displacement

ay1: So-called yield acceleration for the first mode.

Ry1: Correlation dependent on elastic spectral acceleration (Sae(T) and so-called yield acceleration (ay1).

CR1: Spectral displacement ratio.

Sdi1: Nonlinear spectral displacement.

Following the target displacement calculation, a new nonlinear fixed first-mode pushover analysis was performed up to the calculated target displacement to evaluate the building's performance.

3.3.3. Performance Analysis Results for Existing Building

The analysis results obtained at the target displacement of the pushover analysis are presented in Tables 6 and 7. While column rotations remained within the limits of the desired Limited Damage Level (SH) for the DD-2 earthquake level, beam rotations at the mezzanine level exceeded those limits. Notably, these beams were also identified as brittle.

Table 6. Column rotation and shear assessment results at target displacement for DD2 earthquake level

Column Damage Levels					
Storey	Limited Damage	Controlled Damage	Collapse Prevention	Collapse	Total
2	46	0	0	0	46
1	46	0	0	0	46

Column Shear Check			
Storey	Ductile	Brittle	Total
2	46	0	46
1	46	0	46

Table 7. Beam rotation and shear assessment results at target displacement for DD2 earthquake level

Beam Damage Levels					
Storey	Limited Damage	Controlled Damage	Collapse Prevention	Collapse	Total
2	0	6	0	0	6

Beam Shear Check			
Storey	Ductile	Brittle	Total
2	0	6	6

The soil bearing capacity was calculated as 400 kPa. All soil stresses under the foundations were evaluated under both static vertical loads and dynamic lateral earthquake loads, ensuring they remain below the bearing capacity. This analysis confirms that no foundation issues exist for the building.

Furthermore, linear modal analysis under the DD-2 earthquake level established that the building complies with TBEC-2018 requirements regarding storey torsion, soft story, and weak story irregularities. However, the performed story drift check, presented in Table 8, revealed that story drifts exceeding the limits for the desired Limited Damage Level were present.

Table 8. Storey drift check under DD-2 earthquake level

		Drift	Limited Damage Limit	Damage Level
X Direction Displacement	186 mm	0,014	0,01	Controlled Damage
Y Direction displacement	210 mm	0,016	0,01	Controlled Damage
Storey height	13.200 mm			

The analysis has identified potential stability issues within the building structure. While one direction of the building features a pin-connected frame system (Figure 2), the other direction lacks a complete framing system (Figure 1). This deficiency relies solely on girders to connect the individual frames, rendering it susceptible to instability under earthquake loads in this direction.

The assessment analysis revealed that while building columns meet the rotation and shear criteria for the desired Limited Damage Level (SH) under the DD-2 earthquake level, beams do not. Additionally, the building exhibits excessive story drift exceeding the limits for the SH level. This significant displacement, particularly concerning for a building height of 12,0 meters (Figure 2), poses a potential risk of damage to non-structural walls and elements.

Although the observed story drifts comply with the Controlled Damage Level (KH) performance level, the top floor displacement reaches 19 centimeters, potentially leading to substantial damage to non-structural components like walls and equipment. Furthermore, the analysis identified a risk of girder drop-down and damage to roof panels.

Considering these findings and associated risks, the client requested to enhance the structural performance to the Limited Damage Level (SH) as much as feasible. This emphasis on "as much as feasible" acknowledges that achieving the desired performance level surpasses the minimum code requirements (TBEC-2018), but significant improvement is desired despite not being mandatory. Story drifts associated with the Controlled Damage Level (KH) could result in extended repair times, financial losses, and even potential safety hazards. Additionally, the identified stability issues within the building require resolution.

Due to the client's desire to minimize production downtime during the retrofitting process, traditional methods like adding reinforced concrete shear walls, column jacketing, and techniques involving wet concreting, molding, and excavation are unsuitable. Therefore, a retrofit strategy using dampers emerged as the preferred solution. Friction-type dampers were chosen for this purpose, and their application is described in the following section.

4. Retrofitting of the Building

4.1. Analysis Methods

The proposed retrofitting plan, including the application of friction-type dampers, necessitates the use of additional codes alongside the existing TBEC-2018 standard. Since TBEC-2018 does not explicitly address the design and analysis of structures incorporating damping devices, ASCE 7-16 and ASCE 41-17 will be employed as the primary reference codes in tandem with TBEC-2018. This multi-code approach ensures comprehensive guidance for the design and analysis of the damped structure.

The main objectives were;

Linearity of Steel Frame and Connections: Ensure that the steel frame system and connections associated with the damping system remain within the elastic range under the design earthquake forces corresponding to the DD-2 level specified in ASCE 7-16 Section 18.2.1.2.

Overstrength of Steel Frame and Connections: Design the capacity of the steel frame system and connections involved in the damping system to be at least 20% greater than the member demands calculated under the DD-1 earthquake level, as per ASCE 7-16 Section 18.2.1.2. This ensures adequate reserve strength to accommodate potential uncertainties and variations in loading.

Displacement Capacity of Dampers: Design the selected friction dampers to possess a displacement capacity that is at least 30% higher than the maximum displacement experienced by the dampers under the DD-1 earthquake level, adhering to ASCE 7-16 Section 18.2.4.6. This additional capacity provides a safety margin against potential overload scenarios and ensures the long-term functionality of the dampers.

Two earthquake levels were considered for the retrofitted building: DD-2 and DD-1, with each employing a specific analysis method:

DD-2 Earthquake Level: Modeling, analysis, and assessments: These processes were conducted according to TBEC-2018 sections 15 and 5 under the DD-2 earthquake level.

Fixed first-mode nonlinear pushover analysis: This method was chosen due to the structure's behavior satisfying the relevant conditions outlined in TBEC-2018 Section 5.6.2.2. It provides a computationally efficient approach for evaluating the building's global seismic performance.

DD-1 Earthquake Level: Nonlinear time history analysis: This method was selected as the primary analysis technique under the DD-1 earthquake level due to the potential for nonlinear behavior in the structure, including the nonlinearity introduced by the friction dampers.

Linear modal analysis: This method was considered as a permissible alternative if the structure exhibited linear or almost linear behavior. However, in this study, despite the retrofitted structure displaying almost linear behavior, a time history analysis was still performed.

Two earthquake records: To capture the potential variations in seismic loading, two earthquake records were utilized for the time history analysis: Düzce and Erzincan. This approach aligns with recommendations presented in 5ICEES congress papers [9-10], ensuring a comprehensive evaluation of the structure's response under realistic earthquake scenarios.

4.2. Final Retrofitting Studies

4.2.1. Modeling

The proposed retrofitting design for the industrial facility incorporates several key considerations to ensure minimal disruption to operations:

Avoiding Interference with Critical Equipment and Lines: The location of dampers and associated bracing systems was carefully determined to avoid any interference with essential equipment, pipelines, or other important lines within the facility. This involved extensive study and consultation with the client to identify critical areas and ensure that the retrofitting work would not obstruct vital operations.

Minimizing Workflow Disruption: The retrofitting plan was designed to minimize the impact on the facility's workflow. This involved, for example, scheduling construction activities during off-peak hours or utilizing temporary bypasses for critical systems to maintain uninterrupted operation.

Optimized Damper Locations: Following numerous trial studies and discussions with the client, the final locations of the dampers were fixed, as shown in Figures 17, 18, and 19. This optimized placement ensures efficient energy dissipation and improved seismic performance while minimizing the overall impact on the facility's layout and operations.

Damper Selection and Modeling: For the X-direction, 44 pieces of 60 kN dampers were chosen, while for the Y-direction, 52 pieces of 120 kN dampers were selected. The hysteretic, linear, and nonlinear behavior of the dampers was accurately modeled in the Etabs software using plastic Wen spring modeling. This ensured a realistic representation of the damper behavior during the analysis and design process.

Modeling Approach: A linear model with effective stiffness was used for equivalent viscous damping calculations. For nonlinear pushover and nonlinear time history analysis, a bilinear plastic model was employed. This approach provided accurate results while maintaining computational efficiency.

Consistent Load Modeling: Loads, load combinations, and nonlinear hinge properties were modeled in the same manner as described for the existing performance assessment of the structure (refer to Sections 3.1 and 3.2). This ensured consistency and facilitated comparisons between the pre- and post-retrofitted states of the building.

Bracing System Design: Toggle-type steel braces were used to support the dampers in the Y-direction (Figure 20), while diagonal-type steel braces were chosen for the X-direction (Figure 17). This selection was based on considerations of efficiency, ease of construction, and compatibility with the overall structural system. S275 type structural steel was used for the braces and frames.

By carefully considering these factors, the retrofitting design was optimized to achieve the desired performance improvements while ensuring minimal disruption to the functionality of the industrial facility.

An Innovative Retrofitting Technique of an Industrial Prefabricated Building without Evacuation

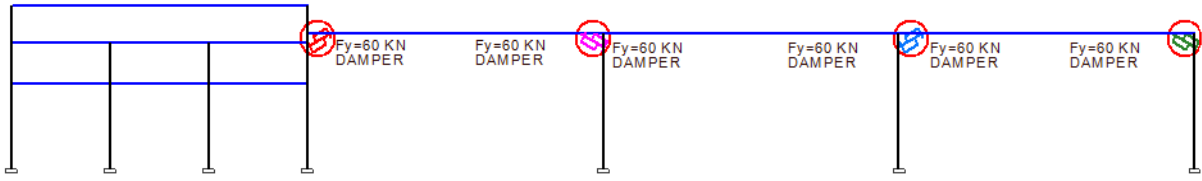


Figure 17. Damper application in X direction (dampers marked with red circles are in a diagonal position close to the top of the columns and between the column and beams)

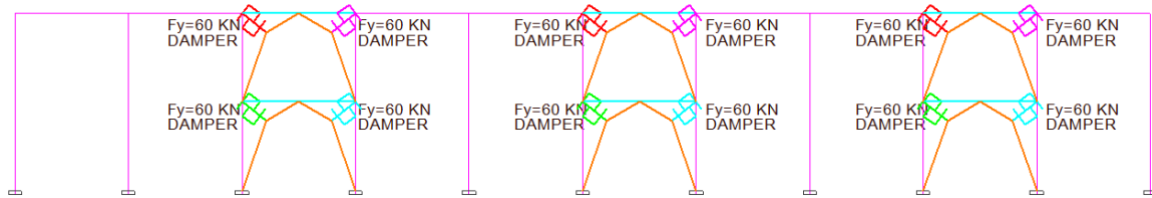


Figure 18. Damper application in Y Direction (dampers are in toggle braces)

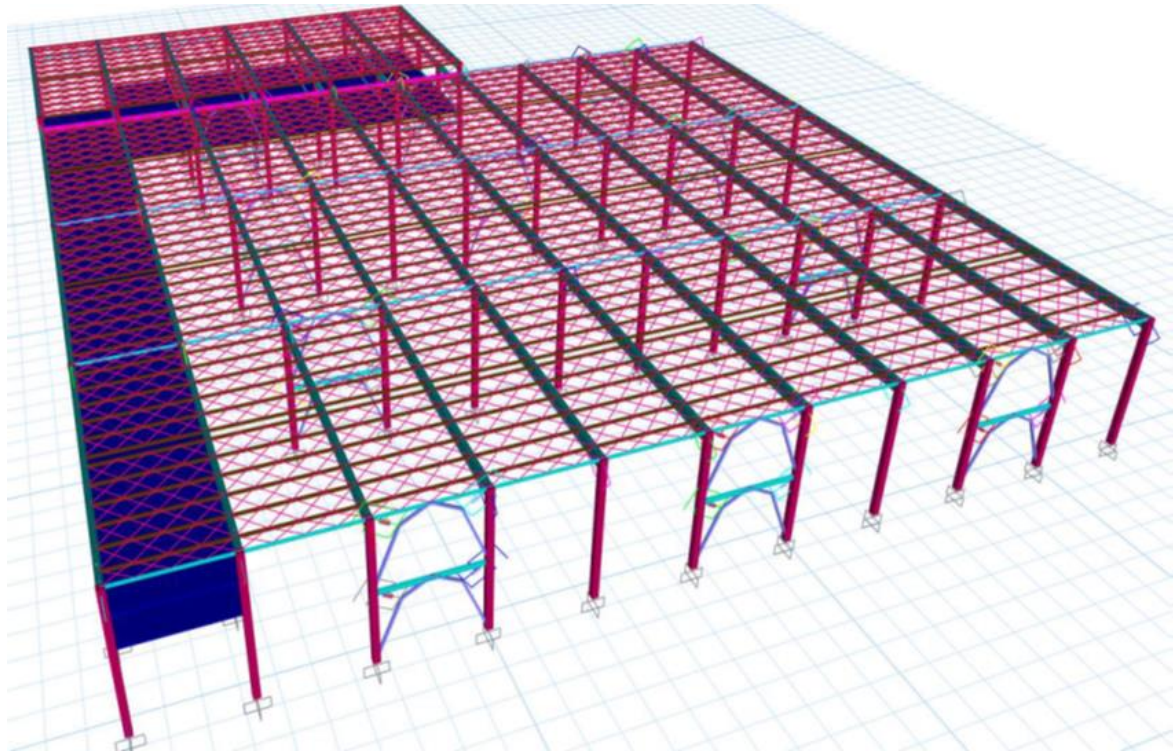


Figure 19. Etabs model view of damper application

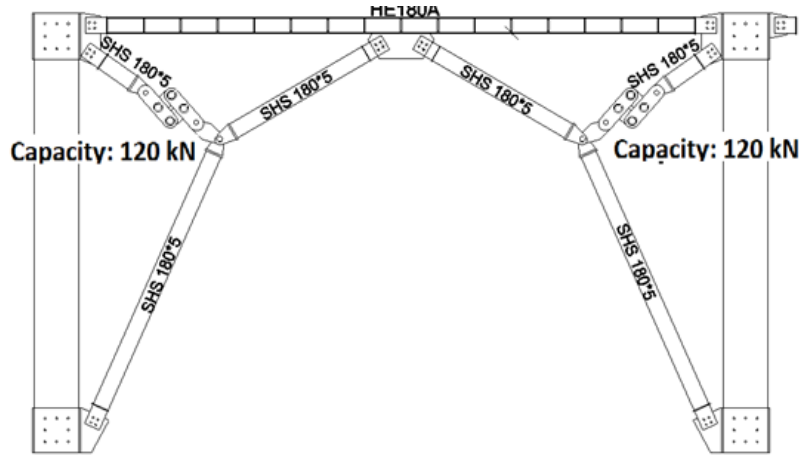


Figure 20. Damper location in toggle type of bracing

4.2.2 Damping Analysis

Equivalent viscous damping calculations were performed for the retrofitted structure using ASCE 7-16 section 18.7.3.2.2 and equations 18.7-47 and 48. The calculated parameters are presented in Table 9.

As intended, the additional damping added to the system through the seismic dampers is higher in the Y-direction (15,8%) compared to the X-direction (6,55%). This is due to the placement of more dampers with higher capacities in the Y-direction.

Consequently, the reduction factors calculated for the X and Y directions are 0,79 and 0,67, respectively. This translates to a 21% decrease in structural demands for the X-direction and a more significant 33% decrease in demands for the Y-direction.

$$\beta_{HD} = q_H (0.64 - \beta_I) \left(1 - \frac{1}{\mu_D} \right) \quad : \text{ ASCE 7-16, section 18.7.3.2.2 equation 18.7-47}$$

$$\beta_{HM} = q_H (0.64 - \beta_I) \left(1 - \frac{1}{\mu_M} \right) \quad : \text{ ASCE 7-16, section 18.7.3.2.2 equation 18.7-48}$$

Table 9. Viscous damping calculation of B1 block under DD-1 and DD-2 earthquake level-linear model

	Initial	Effective
T _x Period (Sec.)	1,808	2,05
T _y Period (Sec.)	0,952	1,398
Equivalent Ductility -X	0,777838	
Equivalent Ductility -Y	0,463724	
Additional Damping -X	0,065538	
Additional Damping -Y	0,158201	

Under DD-1 EQ Level		Under DD-2 EQ Level	
Reduction factor - X	0,79	Reduction factor - X	0,77
Reduction factor - Y	0,67	Reduction factor - Y	0,60

4.2.3 Assessment Analysis of Retrofitted Structure

The assessment analysis of the retrofitted building will be performed following Section 5 of TBEC-2018. This adherence to Turkish codes is essential to ensure the building's compliance with safety regulations.

As the first effective modes of the structure have periods exceeding 70% (Table 10), performing a fixed first mode nonlinear pushover analysis is permissible according to TBEC-2018.

For this analysis, the following key parameters are established:

Seismic mass of the structure: 39.680,23 kN

Spectrum reduction factors:

X-direction: 0,79 (Table 9)

Y-direction: 0,67 (Table 9)

The original earthquake spectrum will be reduced by these factors in both the X and Y directions during the pushover analysis to account for the additional damping provided by the friction dampers. This will ensure a more accurate assessment of the building's seismic performance in its retrofitted state.

Table 10. Mass participation ratios (non-linear model)

Case	Mode	Period (sec)	UX	UY
Modal	1	2,407	0,8811	2,01E-05
Modal	2	1,591	0,0012	0,9056
Modal	3	1,394	0,0156	0,0597
Modal	4	1,063	0,0017	0,0064
Modal	5	0,761	0,0043	0,0085
Modal	6	0,65	0,0003	0,004
Modal	7	0,559	0,0002	0,0002
Modal	8	0,509	0,0462	0,0003
Modal	9	0,491	0,364	3,12E-05
Modal	10	0,409	0,001	0,001
Modal	11	0,401	2,59E-05	2,29E-06
Modal	12	0,388	0,0006	0,0002

A nonlinear fixed first mode pushover analysis was performed for both the X and Y directions of the retrofitted structure to determine the target displacement (Figure 21). This analysis is crucial for evaluating the building's global seismic performance and identifying potential weaknesses. Bilinear plastic springs used to capture the nonlinear behavior of the dampers.

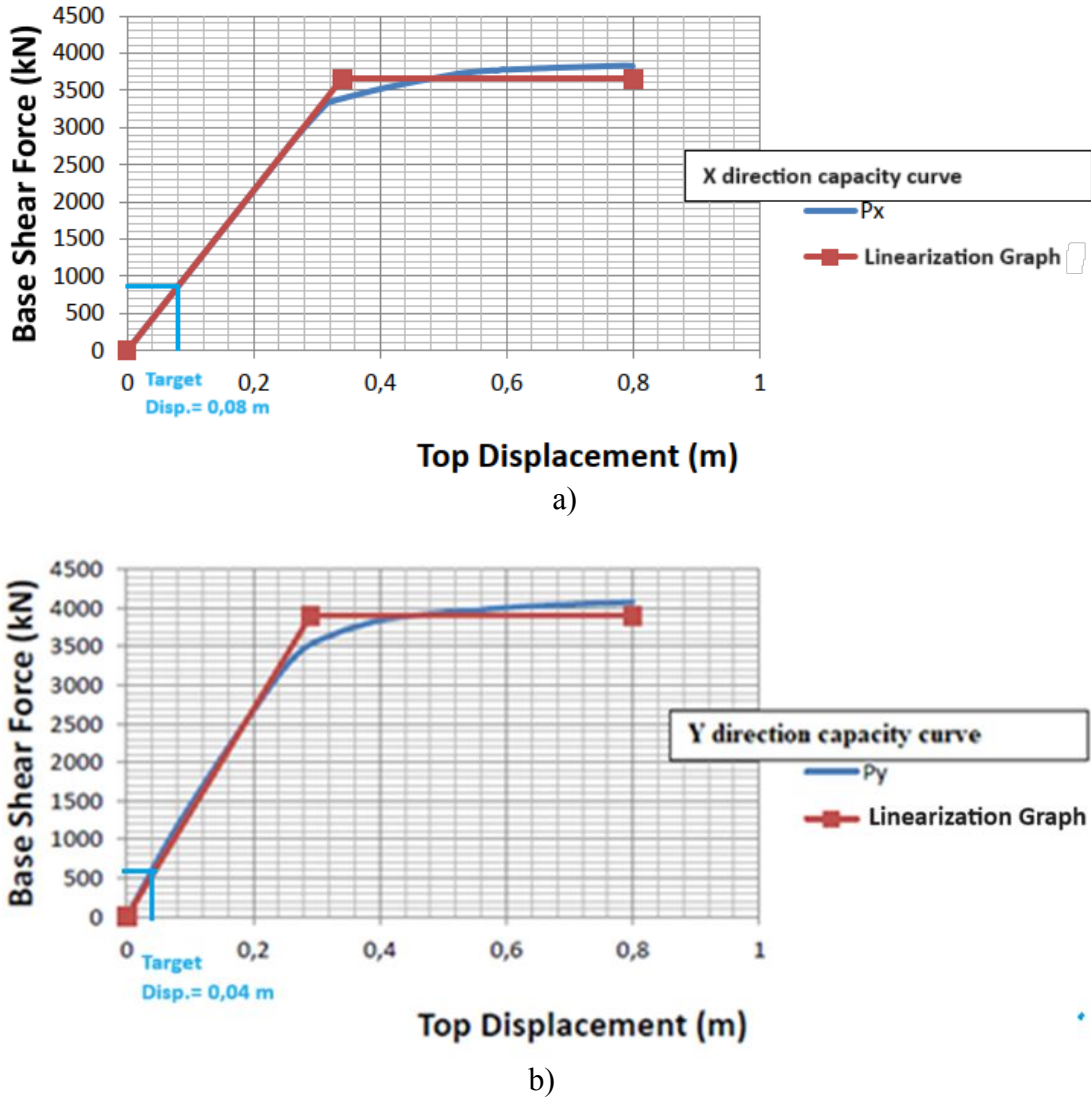


Figure 21. a) X direction push over capacity curve b) Y direction push over capacity curve

Target displacements are determined and presented in Table 11 and inserted in Figure 21. The retrofitted structure is pushed until target displacement using fixed first mode pushover analysis. Demands are obtained at this point, and structure performance is checked.

Table 11. Target displacement calculation of retrofitted structure

Tx (s)	Sae(T)/g	Sae(T)	Sde(m)	ay1	Ry1	CR1	Sdi1	Target Disp. (m) UxN1
2,416	0,055588	0,545316	0,080627	2,817628	0,193537	1	0,080627	0,080627318
Ty (s)	Sae(T)/g	Sae(T)	Sde(m)	ay1	Ry1	CR1	Sdi1	Target Disp. (m) UyN1
1,586	0,0686	0,672968	0,042879	1,347561	0,499397	1	0,042879	0,042878674

In addition to fixed first mode pushover analysis, two time history analyses are performed in order to see the behavior of nonlinear dampers under earthquake (Figure 22).

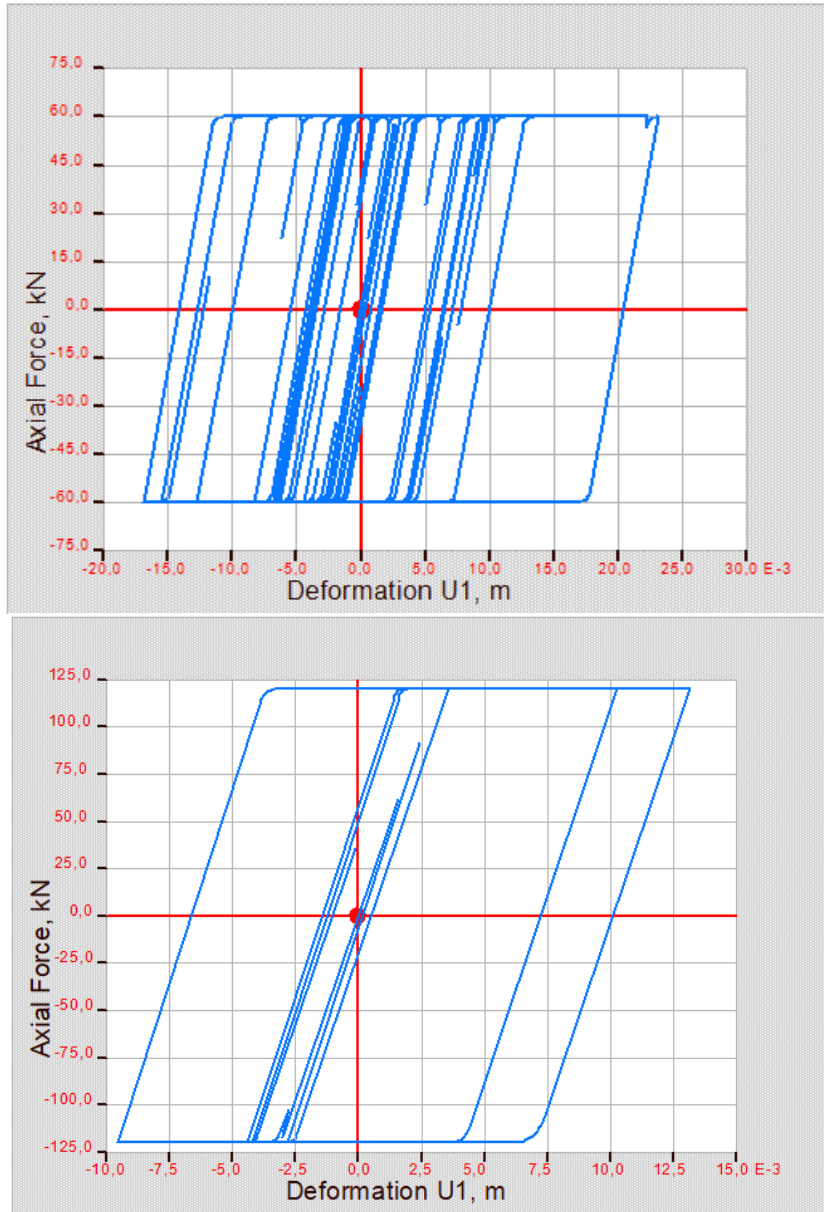


Figure 22. Hysteretic behavior of nonlinear hinges (dampers) 60 and 120 kN under time history analysis

4.2.4 Assessment Analysis Results for Retrofitted Building

The retrofitted structure is re-evaluated using nonlinear fixed first mode pushover analysis up to the target displacement determined in the previous section. re-evaluation considered both DD-1 and DD-2 earthquake levels. The results indicate that all plastic rotations satisfied the SH criteria, confirming sufficient ductility within the primary structural elements for both of the earthquake level (Table 12 and Table 13).

Table 12. Column damage levels and shear check of retrofitted building under DD-1 earthquake level

Column Damage Levels					
Storey	Limited Damage	Controlled Damage	Collapse Prevention	Collapse	Total
2	46	0	0	0	46
1	46	0	0	0	46

Column Shear Check			
Storey	Ductile	Brittle	Total
2	46	0	46
1	46	0	46

Table 13: Beam Damage Levels and Shear Check of Retrofitted Building.

Beam Damage Levels					
Storey	Limited Damage	Controlled Damage	Collapse Prevention	Collapse	Total
2	6	0	0	0	6

Beam Shear Check			
Storey	Ductile	Brittle	Total
2	6	0	6

Story drift checks are carried out for the retrofitted building under DD2 earthquake level;
 X direction displacement: 129 mm, storey drift = $129/13200 = 0,0098$ Limited Damage
 Y direction displacement: 72 mm, storey drift = $72/13200 = 0,0055$ Limited Damage

When drifts of existing and retrofitted structure are compared, it is seen that roof displacement is decreased from 186 mm to 129 mm for X direction (31% decreases) and from 210 mm to 72 mm for Y direction (66% decreases). That means that considerable decrease in non-structural member damages.

Additionally, pin connections of girder-beam and beam-column (Figure 23) are checked for DD-1 earthquake level for overturning and pin failure. They are both determined as safe for retrofitted buildings.

An Innovative Retrofitting Technique of an Industrial Prefabricated Building without Evacuation

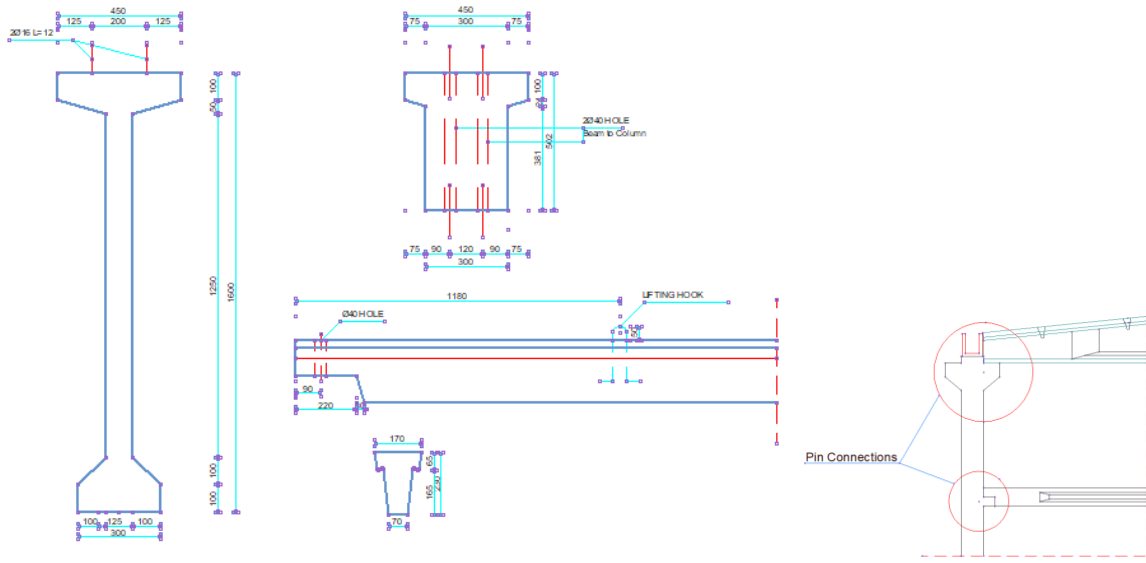


Figure 23. Pin connection of girder to beam and beam to column

Foundation Stress Check: Stresses under the foundations were analyzed and found to be less than 400 kPa, which satisfies the soil-bearing capacity. This confirms that the additional loads introduced by the retrofitting measures and seismic loads do not exceed the soil's capacity, ensuring the stability of the foundation system.

The effectiveness of the dampers is checked using DUZCE earthquake scaled for DD-2 level. Displacements are seen as significantly decreased for X and Y directions (Figure 24, Figure 25).

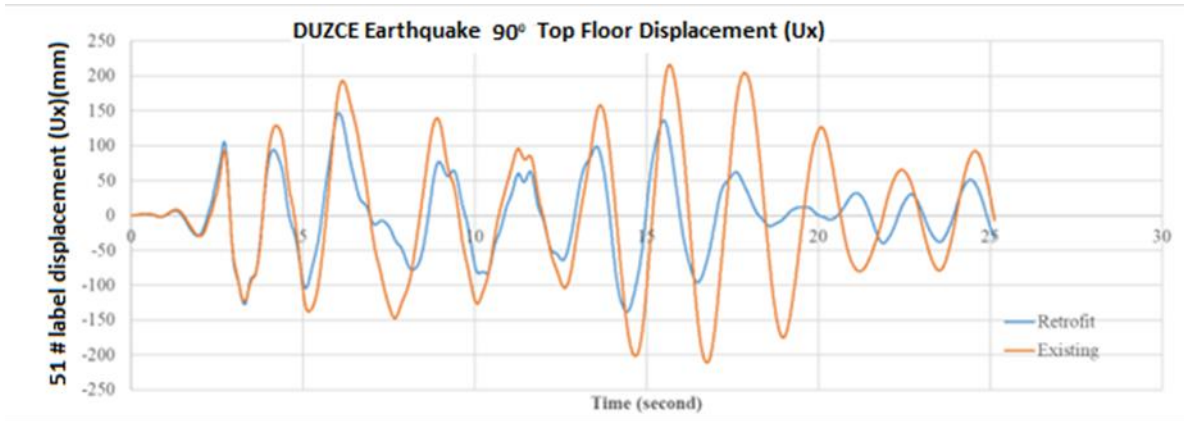


Figure 24. X direction top floor displacement for DD-2 scaled Duzce earthquake

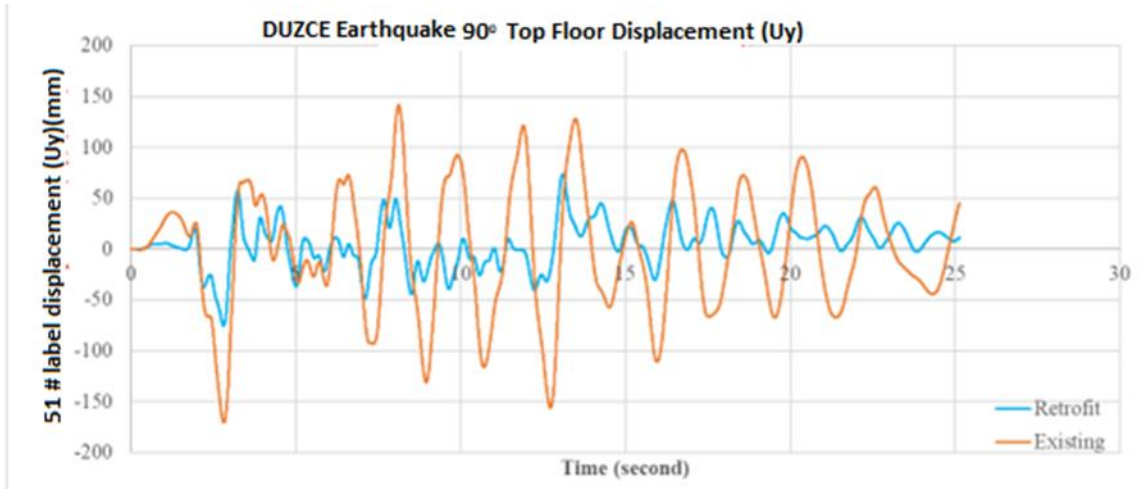


Figure 25. Y Direction top floor displacement for DD-2 scaled Duzce earthquake

Another important mutual problem of B1 and B2 blocks were pounding each other during the earthquake due to insufficient dilatation space between two adjacent blocks (Figure 26).

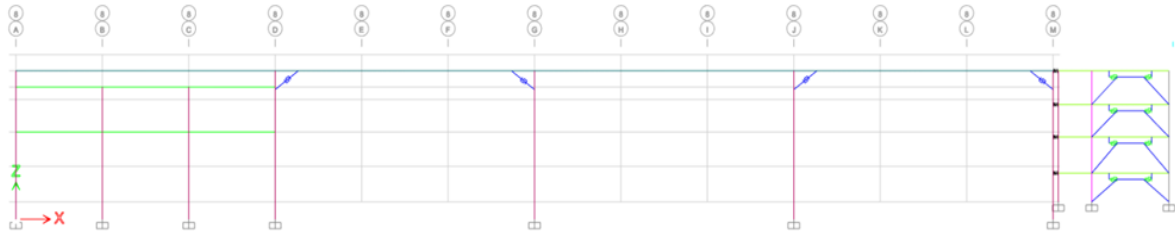


Figure 26. B1 and B2 blocks adjacent to each other

X-direction displacement of Block B1 decreased to 129 mm after retrofitting with dampers, but it still exceeds the existing space of 50 mm between the two blocks. This discrepancy suggests a potential for pounding to occur during seismic events. To further investigate this concern, a time history analysis was performed. For this purpose, inelastic spring HERTZ modeling is preferred and gap members are modeled between two adjacent blocks as seen in Figure 27.

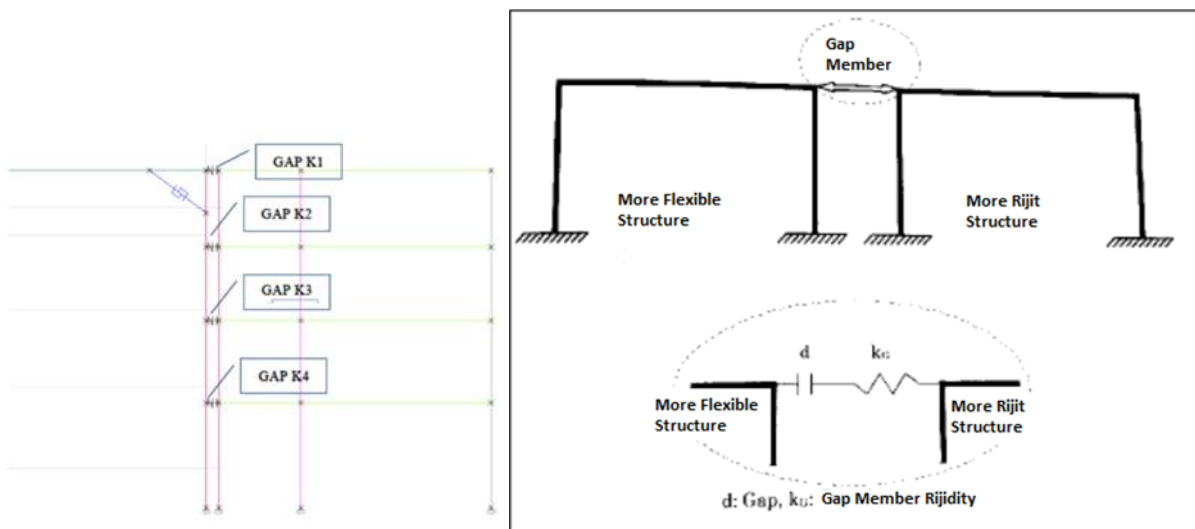


Figure 27. Gap member modeling in Etabs.

Pounding force – Displacement relationship of the Hertz modeling is given as:

$$f = \begin{cases} K(d - open) & \text{if } d - open < 0 \\ 0 & \text{otherwise} \end{cases} \quad (1)$$

After time history analysis, pounding forces obtained as a function of time and force can be seen in Figure 28.

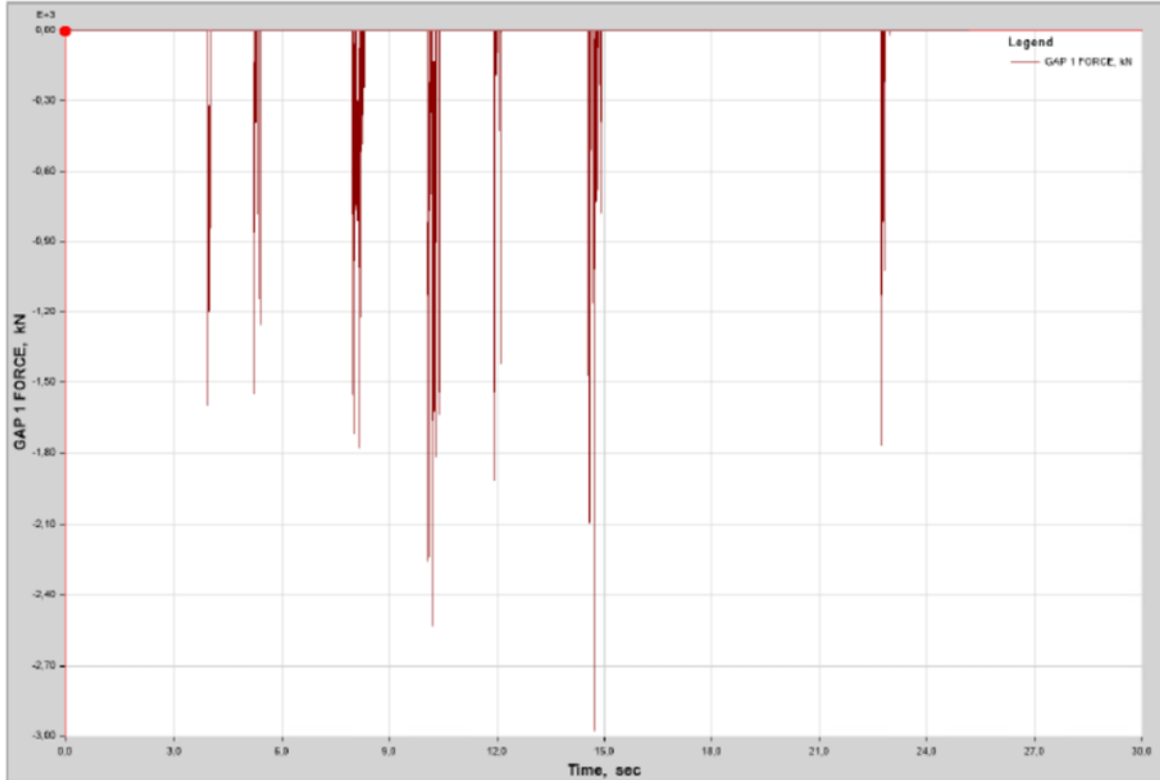


Figure 28. Pounding forces obtained in time history analysis

Demand-capacity ratios for the columns under pounding forces were checked and found to be acceptable, with a maximum value of 1.5 (Figure 29). This indicates that the columns have sufficient capacity to withstand the pounding forces without exceeding their yield strength. This represents a significant improvement compared to the pre-retrofitting state, where the demand-capacity ratios due to pounding forces were significantly higher, reaching 4-5. This confirms that the increased damping provided by the friction dampers effectively addressed the pounding issue, ensuring the safety and stability of both blocks during seismic events.

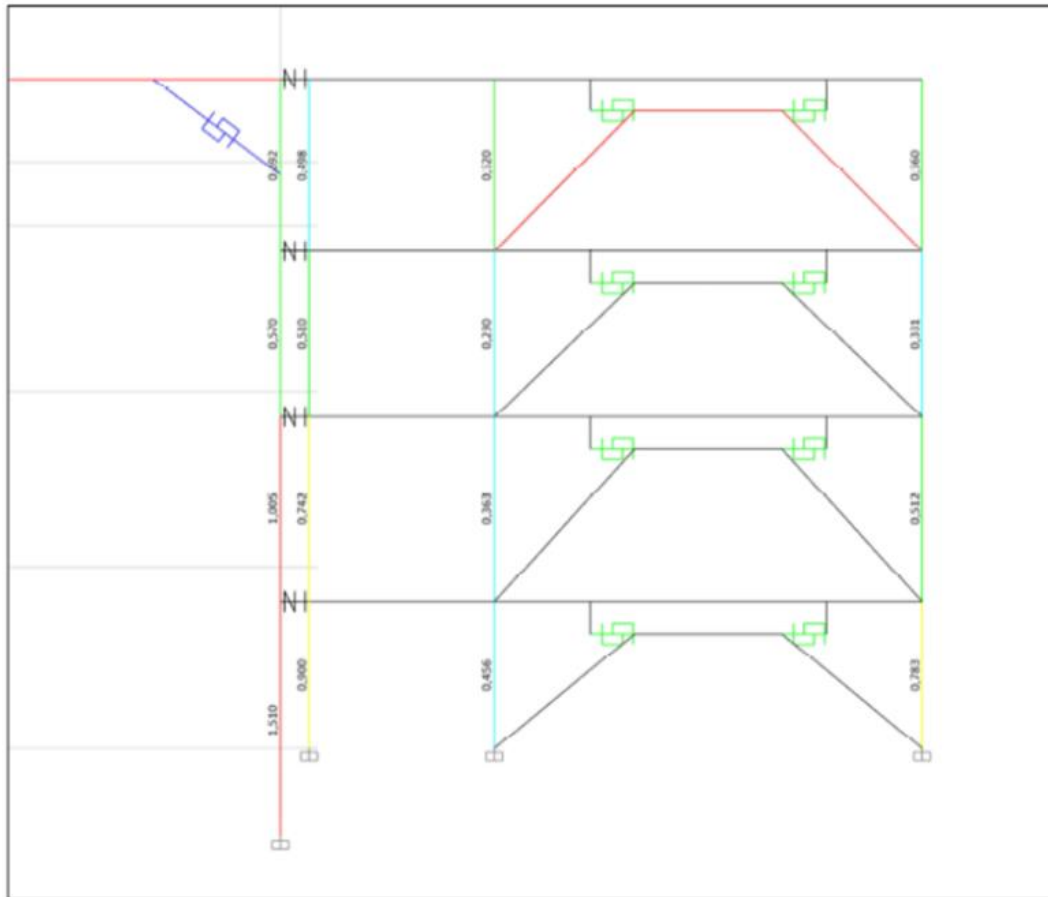


Figure 29. Demand capacity ratios of two blocks under pounding forces

5. Results

Original Performance:

Controlled Damage Level under DD-2 earthquake level (as per TBEC-2018).

Brittle behavior observed in some beams.

High story drifts causing potential damage to non-structural members.

Pounding problem identified between adjacent blocks.

Retrofitted Performance:

Upgraded to Limited Damage Level under DD-2 earthquake level.

All columns and beams exhibit ductile behavior.

Significant reductions in roof displacement:

X-direction: 31% decrease (186 mm to 129 mm).

Y-direction: 66% decrease (210 mm to 72 mm).

Pounding issue between blocks solved by increased damping.

Pin connections for girder-beam and beam-column deemed safe for DD-1 earthquake level.

Retrofit installation completed without disrupting building operations.

Key Benefits of Retrofitting:

Improved seismic performance and safety.

Reduced risk of damage to both structural and non-structural elements.

Enhanced occupant comfort and building functionality.

Mitigation of pounding problem between adjacent blocks.

Minimal disruption to building operations during retrofitting.

6. Conclusions

The implemented retrofitting measures, particularly the friction dampers, demonstrably improved the seismic performance of the precast building. By successfully addressing the identified deficiencies, the retrofitting project ensured the building's compliance with the desired Limited Damage Level and enhanced its resilience against earthquake loads. This case study highlights the effectiveness of friction dampers as a viable solution for improving the seismic performance of existing prefabricated structures.

Retrofitting installation works are performed without stopping the functionality of the Building with some safety precautions and slight separations (Figure 30).



Figure 30. Installation photos

Author Contributions

Suat Yıldırım and Yüksel İlkey Tonguç both contributed to the design and implementation of the research, to the analysis and the evaluation of the results.

Conflict of Interest

Authors declare no conflict of interest.

References

- [1] TBEC-2018- Turkish Building Earthquake Code
- [2] ASCE 41-17 Seismic Evaluation and Retrofit of Existing Buildings; American Society of Civil Engineers: Reston, VA, USA, 2017.

- [3] ASCE 7-16 Minimum Design Loads and Associated Criteria for Buildings and Other Structures 2017
- [4] Ersoy, U., Özcebe, G. and Tankut, T., (2000), 1999 Observed damages of precast structures in Marmara and Düzce Earthquakes. 10. Prefabrication symposium book page 1, Istanbul
- [5] Özmen, G., Yüzügüllü, O, and Zorbozan, M., (1997), Evaluation of TBEC-2018 for prefabricated structures. Turkish Earthquake Foundation publications. TR 97-006, Istanbul.
- [6] Palancı.M and Şenel Ş.M.” Rapid seismic performance assessment method for one story hinged precast buildings” Structural Engineering and Mechanics 48(2) 257-274 (2013).
- [7] Cahit Gürer Kocatepe University Yapı Teknolojileri II.
- [8] Etabs Ver.18 : A finite element based structural analysis software published by CSI (Computers & Structures Inc.) based on North California. Please refer to www.csiamerica.com for detailed information.
- [9] Erkuş B, Yıldırım S, Güler M.D., Özer C, Sütçü F, Alhan C. (2019) Seismic design of structures with dampers, part II: A proposal for design basis for applications in Turkey. 5th International Conference on Earthquake Engineering and Seismology (5ICEES).
- [10] Yıldırım S., Güler M.D., Özer C., Sütçü F., Alhan C. ve Erkuş B. (2019) Seismic design of structures with dampers, part I: review of international standards. 5th International Conference on Earthquake Engineering and Seismology (5ICEES).



© 2024 by the authors. Submitted for possible open access publication under the terms and conditions of the Creative Commons Attribution (CC BY) License (<http://creativecommons.org/licenses/by/4.0/>).




Research Article

Academic Platform Journal of Natural Hazards and Disaster Management
5(1), 30-45, 2024 DOI: 10.52114/apjhad.1434612



Cloudbursts Strike over Foothills Himalaya of Uttarakhand, India: A Case Study from Maldeota, Dehradun District

Sushil Khanduri ^{1*} 

¹KainGeotech Pvt. Ltd., Dehradun-248001, India

Received: / Accepted: 16- February-2024 / 11-June-2024

Abstract

The present study highlights the cloudburst issues that occurred in Raipur region of Maldeota area in Dehradun City. On the night of August 20, 2022, this area of Uttarakhand state capital Dehradun was lashed by high-intensity rainfalls or cloudbursts resulting in the water level of sub-watersheds of the Song river rising enormously, particularly Bandal *Nadi* and Song *Nadi*. Bhaishwar and Sarkhet villages which are situated on the Bandal valley came into the limelight due to loss of human lives and property. 5 people died while 3 people injured and 24 animals lost whereas about 8.25 hectares of agricultural fields were damaged and 12 families were rendered homeless in these incidences. Transport connectivity of the Sarkhet and adjoining areas have been disrupted due to roads being washed away at many places. Geologically, the devastated area is observed to be fragile due to its proximity to the Main Boundary Thrust (MBT) and subsequent Fault as well as its location to the Eastern fringe of the Mussoorie Syncline. It was also noticed that untraditionally ways of habitation patterns and economic opportunities due to increasing tourist inflow in the area are responsible for the enhanced devastating potential of disaster. The purpose of this research is to ascertain the actual causes and impacts of the disaster and the feasibility of rehabilitation land for homeless families. This work mainly concentrates on current risk scenarios that may be reflected in the future and suggestive measures to reduce its impacts within the area.

Key words: Causes, Debris flow, Flash food, Impacts, Lesser Himalaya, Risk mitigation

1. Introduction

In recent decades, extreme weather events like high-intensity rainfalls or cloudbursts have become more frequent worldwide that are attributable to climate change (1-4). This led to flash floods in many countries causing huge loss of life, property and infrastructure along with geo-environment and economic damage (5-9). Human interference in the form of untraditional ways of habitation patterns and infrastructural developments over fan materials of the local streams and over alluvial terraces or low-laying areas of major streams are mainly responsible for the disaster. However, we always get information about such incidents/disasters from the local inhabitants of the area or media persons. At present, despite having sufficient resources, we are not able to accurately predict high-intensity rainfalls or cloudbursts. We still need to do in-depth research in this area to safeguard against the same in the future.

According to Indian Meteorological Department (IMD), downpour of 100 mm occurs within a shorter duration over an area of 20-30 sq. km, is defined as a cloudburst. Such events are

* Corresponding Author e-mail: sushil.khanduri@gmail.com

unpredictable in nature because they are controlled by distinguished geomorphic and physiographic parameters and generally occur in elevation ranges from 1200 to 2200m in the hilly region (10). Most often, cloudbursts trigger over the higher reaches of Ist and IInd order streams, especially during the monsoon season in the early morning hours cause debris flows through local streams while flash floods through major streams. These observations were confirmed by analysis of 50 cloudburst events in the Upper Alaknanda Basin (11-12).

Uttarakhand, a Central Himalayan state located in the Indian subcontinent, consists of 13 districts, which is well known for its vulnerability to natural hazards such as landslides, earthquakes, floods, avalanches, glacial lake outburst floods and flash floods (13-16). In recent times, with changes in climate due to global warming across the world, the state regularly faces extreme events not only during monsoon, but also in pre-monsoon and post-monsoon periods. Analysis of last 52 years of data of heavy localized precipitation or cloudburst-like events in the state of Uttarakhand from 1970 to 2022 shows that the majority (31%) of such events occurred in the month of August, while 28% were recorded in the month of July and 11% recorded in September month. This was followed by 7%, 9% and 14% incidences that occurred in the months of May, June and October respectively (Figure 1). Mostly, such events were concentrated in Pithoragarh, Chamoli, Uttarkashi and Rudraprayag districts, while slightly fewer than those were observed in Bageshwar, Tehri and Pauri Garhwal districts and very few incidents were reported in Nainital, Almora, U.S. Nagar and Champawat districts (17-19).

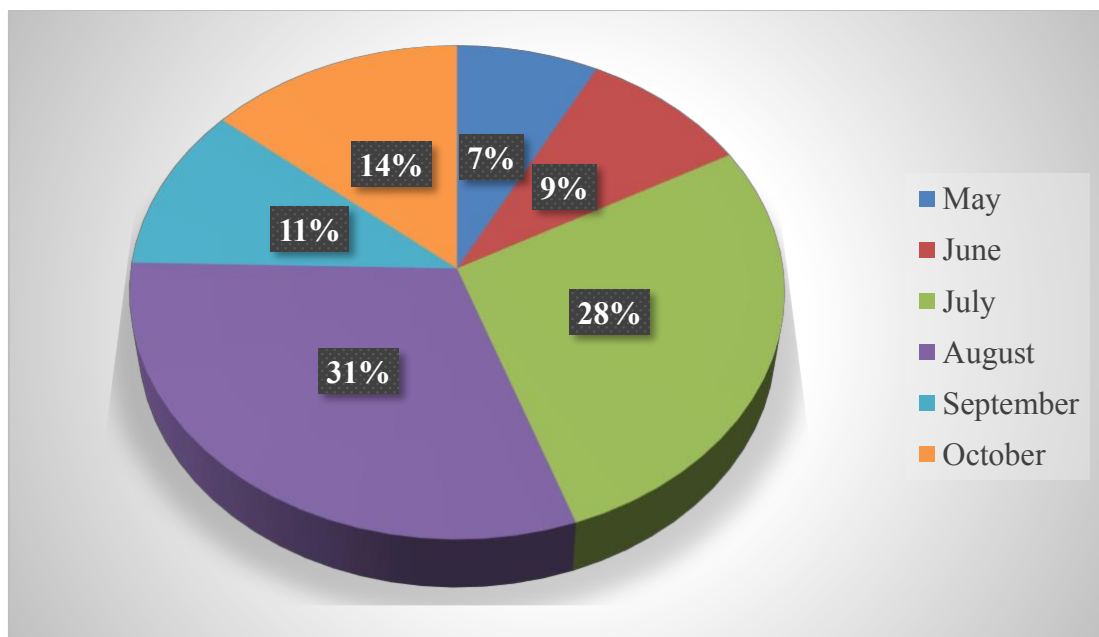


Figure 1. Month-wise percentage of heavy localized precipitation or cloudburst-like events from 1970 to 2022 in the state of Uttarakhand Himalayas (17-19)

In the last decade, high-intensity rainfall or cloudburst incidences have happened at various places in the state of Uttarakhand wherein killing more than 4000 people and destroying settlements together with huge economic and environmental damage. Losses incurred in these catastrophic events are confirmed by Table 1. This region received unusually high-intensity rainfalls between October 17 and 19, 2021, especially over Nainital, Champawat, Udham Singh Nagar, Pithoragarh, Bageshwar and Almora districts. This led to several landslides and flash floods causing loss of 72 lives (18). This makes it clear that high-intensity rainfall in October is a result of the impact of climate change.

Cloudbursts Strike over Foothills Himalaya of Uttarakhand, India: A Case Study from Maldeota, Dehradun District

Table 1. Losses incurred in heavy localized precipitation or cloudbursts ensured debris flows and flash floods in Uttarakhand (17-19)

Sl. No.	Year of occurrence	Incidence and human loss
1.	August 3, 2012	35 people died in flash flood caused by cloudburst in Asi Ganga, a tributary of Bhagirathi river in Uttarkashi district
2.	September 13, 2012	Cloudburst ensured debris flows in Okhimath town of Rudraprayag district, killing 69 people
3.	June 16 & 17, 2013	Cloudburst & GLOF ensured flash floods in Mandakini valley, killing 4127 people
4.	July 01, 2016	22 people died due to debris flows generated by cloudburst in Bastari and Naulra of Didihat tehsil in Pithoragarh district
5.	August 14, 2017	Excessive heavy rainfalls or cloudbursts ensured flash floods in the catchment areas of Kali river, especially Simkhola Gad and Malpa Gad respectively at Mangti and Malpa in Dharchula tehsil of Pithoragarh district, killing 27 persons
6.	August 18, 2019	21 people died around the Arakot in the flash flood caused by cloudbursts in Khaneda Gad, a tributary of Pabber river in Mori tehsil of Uttarkashi district
7.	July 20, 2020	11 people died at Tanga Village due to cloudburst ensured debris flows in a 1 st order stream in Pithoragarh district
8.	July 18, 2021	Extremely rainfalls or cloudbursts in Mando Gadhera, a tributary of Bhagirathi river, killing 4 people at Mando village in Uttarkashi district,
9.	August 27, 2021	A cloudburst like incidence took place in Jumma Gad, a tributary of Kali river, in which 7 people died at Jumma village in Dharchula tehsil of Pithoragarh district,
10.	August 20, 2022	Cloudburst ensured flash flood and debris flows in Bandal <i>Nadi</i> and its sub-watersheds at Sarkhet and Bhiswar villages of Raipur region in Maldeota area of Dehradun district, resulting in death of 5 people

Earlier, on August 13, 2018, a rock fall/slide triggered on a local stream, a tributary of Bandal *Nadi* that blocked its course for 7 hours creating a lake dimension of 150 m long and 40 m with 3-5m deep at Timli sain *tok* of Lwarkha village in Tehri Garhwal district. Initially, this incidence created panic in downstream settlements, but after 7 hours lake water gushed out through a detached rock mass and drained normally (20).

Except that, on February 7, 2021, 204 people died in the flash flood of Rishiganga and Dhauli Ganga during winter season in Chamoli district of Uttarakhand, which attracted worldwide attention (21). Subsequently, Joshimath town in Chamoli district also faced serious land subsidence in August 2022, due to which some property and infrastructure were seriously affected, while in January 2023, more than 500 houses were severely damaged, which again attracted worldwide attention (22-23). Due to the accelerate subsidence, 81 ground cracks were recorded and the highest number of ground cracks were observed in Manohar Bagh and Singdhar areas along with damage to civil structures in the same localities. The vertical settlements of giant boulders results from removal of fine materials embedded with the same due to the piping of subsurface water flows (24).

Recently on August 20, 2022, high-intensity rainfall or cloudburst-like incidences occurred in the upper catchment of Song river, particularly in the Bandal *Nadi*. Sarkhet and Bhaiswar villages situated over the fan materials of IInd order streams, a tributary of Bandal *Nadi*, were badly affected due to water-saturated debris flows in the same, killing 5 people. Additionally, flash floods through the Bandal *Nadi* caused devastation across the valley, wherein several property and infrastructure were badly damaged and some of those wiped out.

In view of high damage in Bandal valley, this area has been taken up for the present study. The main objectives of the study area include (i) to delineate geological and geomorphological influences in the devastated area; (ii) identifying places where damage to property and infrastructure has occurred; (iii) to demarcate the places where streams have changed their course, (iv) feasibility of rehabilitation land for homeless families of Sarkhet and Bhaiswar villages, (v) to find out the actual causes of damage and distraction, and (vi) assessment of current risk scenario which may be reflected in future and suggested measures to mitigate future impacts.

2. Materials and Methods

2.1. Study Area

Dehradun district is situated in the northwestern corner of Uttarakhand and covers an area of 3088 sq.km at an altitude of 640 m above mean sea level. The district is bounded by Uttarkashi district on the North, Tehri Garhwal and Pauri Garhwal districts on the East, Saharanpur district (UP) in the South and its southern tip touches the border of district Haridwar. Its western border connects to Sirmour district of Himachal Pradesh which is separated by Tons and Yamuna rivers. According to Seismic Zoning Map of India, this area falls in Zone-IV (25).

Delhi, the capital of India is located about 235 km from Dehradun city. Moreover, the famous hill station of tourist destination Mussoorie is situated just 30 km from Dehradun. Dehradun district consists of six Development Blocks as Chakrata, Kalsi, Vikasnagar, Sahaspur, Raipur and Doiwala. The district is well connected to all major cities of North India by rail, road network and airways. The nearest airport is Jolly Grant which is located about 24 km from this City.

The climate of Dehradun is more temperate and humid than the surrounding districts. Not only at higher altitudes in this region, but even in Dehradun during winter the temperature drops below the freezing point and reaches 40°C in Summer. Higher mountains are covered with snow during the winter. The total annual rainfall is about 1800 mm, most of which occurs in the months of July- August. Within the limits of the district are the high peaks of the Outer Himalayas as well as the Doon valley, whose climatic conditions are almost similar to those of the plains.

The devastated Bandal *Nadi* comes under Survey of India Toposheet No. 53 J/3 and is located in the North of the Raipur area (Figure 2). This area was devastated by flash floods associated with high-intensity rainfalls or cloudbursts on August 20, 2022. The devastated Bhaiswar village is situated on the right bank of the southwesterly flowing Bandal *Nadi* and is about 10km from Raipur town on Maldeota-Dhanolti motor road. The habitation of this village is placed on fan materials of southerly flowing Musniwala *Nallah* which is a IInd order seasonal stream, a small tributary of Bandal *Nadi* in the area. Another devastated Sarkhet village is also situated on a IInd order seasonal stream and is around 3 km downstream of Bhaiswar village on the right

Cloudbursts Strike over Foothills Himalaya of Uttarakhand, India: A Case Study from Maldeota, Dehradun District

bank of Bandal *Nadi*. 10 families from Sarkhet village and 2 families from Bhaishwar village, a total of 12 families were rendered homeless due to the destructive debris flows into these streams. Rehabilitation land whose feasibility has been done, is located southwest of Sarkhet village at a distance of about 4 km from the PPCL mine area on the Silla-Kyara motor road.

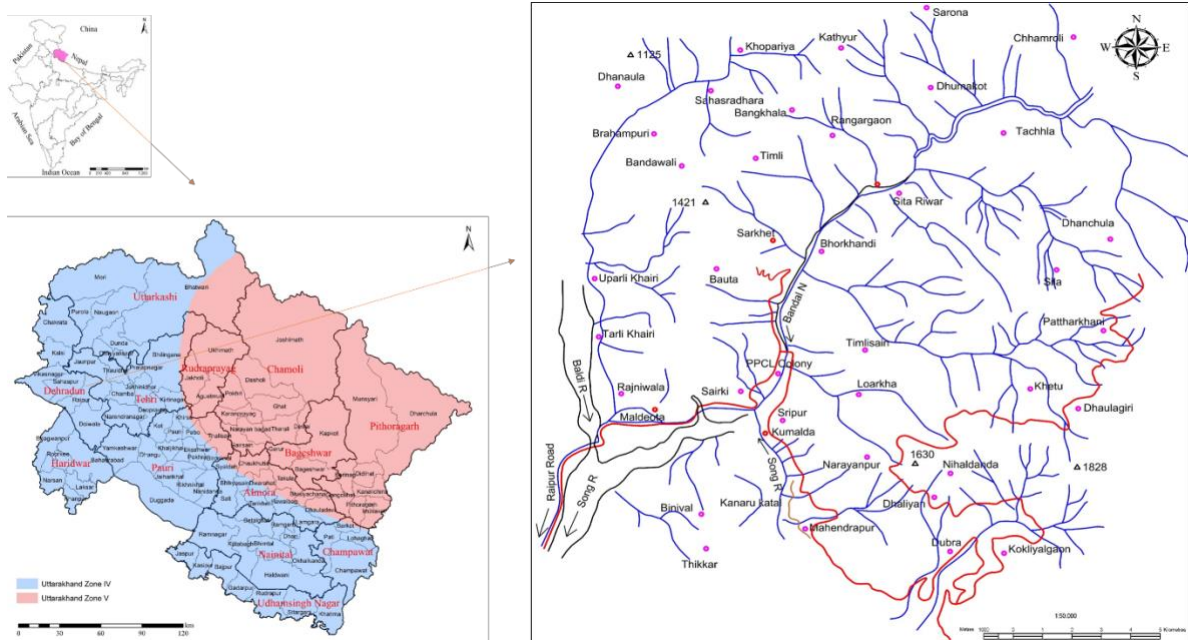


Figure 2. Location map of the study area. On the left side, Uttarakhand map shows earthquake zones (25)

2.2. Data and Approach

A detailed ground investigation has been conducted in the study area to ascertain the actual causes of damage, such as morphometric changes, affected settlements and infrastructures. Feasibility of rehabilitation land has also been verified through on-site inspection. Geological and tectonic inferences are updated based on previous records and ground truth.

- I. Survey of India toposheet No. 53 J/3 at a scale of 1:50000 has been utilized for understanding physical factors of the area, such as slope, drainage, elevation and topography and also utilizing for preparing location map of the devastated area.
- II. Handheld Global Positioning System (GPS) has been used for precise geolocation of morphometric changes and damage to property and infrastructure.
- III. Google Earth Pro satellite image has been utilized to measure distances of locations where changes in stream course have occurred.
- IV. ArcMap 10.5 and AutoCAD 15 software were used to prepare thematic maps of the study area.

3. Geological Setting

Geologically, a sequence of sandstone and mudstone of the Siwaliks mountain range of the Outer Himalayas are observed in the devastated area which has juxtaposed along the northeast dipping Main Boundary Thrust (MBT) along with the sequence of phyllite and quartzite of the Lesser Himalayan mountains. This metamorphic succession of the Jaunsar Group comprising the Chandpur and Nagthat formations is overlain by a large unconformity by the sedimentary succession of the Blaini, Krol and Tal formations of the Mussoorie Group. Rocks comprise

quartzite, shale, slate, phyllite, siltstone, dolomitic limestone/limestone, diamictite, conglomerate etc. (26-29). The MBT is disrupted by the presence of the N-S trending Baldi-Song Fault near Raipur area (29).

The rocks of 'Mussoorie Syncline' are folded into a doubly plunging syncline, with its axis trending in general NW-SE direction in the form of several culminations and depressions are also noticed in the devastated area. Sedimentation pattern is often interpreted as evidence of the progressive rise of the Himalayas and recent onset of tectonism along the MBT (30-31). The greater part of the valley area is occupied by the Dehradun and Bhogpur fans in the South (32), deposited by the rivers flowing from Lesser Himalaya and influenced by the activity of MBT and associated faults. The lithostratigraphic succession of the area is given in Table 2.

Table 2. Lithostratigraphic succession of the devastated region (26-29)

Group	Formations	Lithology	Age
Mussoorie	Tal	Quartzite, phosphoritic pyriterous shale/slate, chert and siltstone	Cambrian
	Krol	Dolomitic limestone/Limestone with interbedded shale	
	Balini	Diamictite, conglomerate, Slate and boulder bed	Neoproterozoic
Jaunsar	Nagthat	Quartzite, shale, phyllite and conglomerate	
	----- Unconformity -----		Paleoproterozoic
	Chandpur	Phyllite, dolomite with basic intrusives	
----- Main Boundary Thrust(MBT) -----			
Upper Siwaliks	Boulder conglomerate	Coarse boulders, conglomerates with friable sandstone and clay	Late Pliocene to Early Pleistocene
Older Alluvium	Doon Gravels	Brown silt, clay, sand, pebble and boulders	Middle to late Pleistocene
Newer Alluvium	Channel Alluvium	Grey Sand, silt and clay	Holocene

4. Geomorphology and Physiography

Dehradun is an intermontane longitudinal tectonic synclinal basin bounded by Faults and is delimited by Main Boundary Thrust (MBT) in the North (26, 30, 33-36). The Ganga River demarcates its eastern boundary which flows along NE-SW trending Ganga Tear Fault, while the Yamuna River flowing along N-S oriented Yamuna Tear Fault limits its extension in the west and the southern boundary, demarcated by Himalayan Frontal Thrust (HFT).

Physiographically, the devastated area represents the high rugged mountainous terrain of Lesser Himalayas in the North, with U & V-shaped valleys and high rising steeply sloping hill ranges, while the Piedmont fans and Doon Valley lie in the southern part. Longitudinal ridges, transverse ridges and intermittent deeply dissected valleys are common features of this region. The Doon Valley is a synclinal depression between the Lesser Himalayan terrain in the North and Sub-Himalayas in the South. Aligned parallel to general trends of the Himalayas, it is a veritable intermontane valley, the floor of which is filled with thick detritus shed from overlooking hill slopes.

The southerly flowing Song river forms the main drainage in the region and is joined by its major tributaries Bandal *Nadi*, Song *Nadi* and Baldi River. Bandal *Nadi*, affected by flash floods, originates from the Sidh-Ki-Dhar (2519 m) of Dhanaulti in Mussoorie region. Initially, it flows from NW- SE direction which turns near the Bharmakhal, after that it flows from NE – SW direction and joins the northwest flowing Song *Nadi* at Kumalda village (745 m). Thereafter, the Song river flows in approximately E-W direction and meets the southern flowing Baldi river at Asthal, and ultimately becomes known as the Song river. The overall drainage pattern of the area is dendritic. The Baldi and Bandal sub-watersheds are semi-circular in nature and the area is characterized by high to moderate relief and the drainage system is structurally controlled (37).

4.1. Morphometric Changes

Alluvial terraces were observed at Dhantu Sera, Bhaiswar, Sarkhet, Maldeota, and Kumalda whereas fan material of seasonal streams was also observed, especially at Sarkhet and Bhaiswar villages in Bandal *Nadi* valley during the field visit. On August 20, 2022, high-intensity rainfalls or cloudbursts resulted in high sediment laden discharge in Bandal *Nadi* along with its all tributaries, causing extensive damage in the areas where these materials resided. Alluvial terraces along the Bandal *Nadi* were also severely eroded resulting in agricultural fields together with property and infrastructure being badly damaged or destroyed. Due to severe bank erosion, Bandal *Nadi* has significantly changed its course at many places and has widened its channel. Details of the places where the stream changed its course are tabulated in Table 3.

Table 3. Details of the places where the stream has changed its course

S. No.	Stream	Location	Change in stream course (in meters)	Change in stream bank (Left/Right)
1.	Bandal <i>Nadi</i>	Dhantu Sera	13-18	Left Bank
2.		Between Bhaiswar and Dhantu Sera	20-35	Right Bank
3.		Sarkhet	10-15	Right Bank
4.		Opposite Granny's Den Resort	6-12	Right Bank
5.		Doon Defence College area	18-35	Left Bank
6.		Red Bridge/Laal Pull	10-16	Right bank
7.		At Kumalda	8-18	Left Bank
8.	Song River	Four Banyan Spirits and Nature Resorts	15-55	Right Bank

4.2. Losses and Damages

Raipur region of Maldeota area received extremely heavy rainfall during the late night of August 19, 2022 and early morning of August 20, 2022, due to which the water level of the tributaries of Song River, particularly the waters of Bandal *Nadi* and Song *Nadi* to rise as much as 3-4m above the danger level. This led to erosion of its banks resulting in widespread devastation in the area. Numbers of property and infrastructure were severely damaged at Sarkhet, Bhaiswar, Sairki, Chhamroli and Maldeota areas, while some of these were washed away in flash flood and debris flow incidences.

Cloudbursts Strike over Foothills Himalaya of Uttarakhand, India: A Case Study from Maldeota, Dehradun District

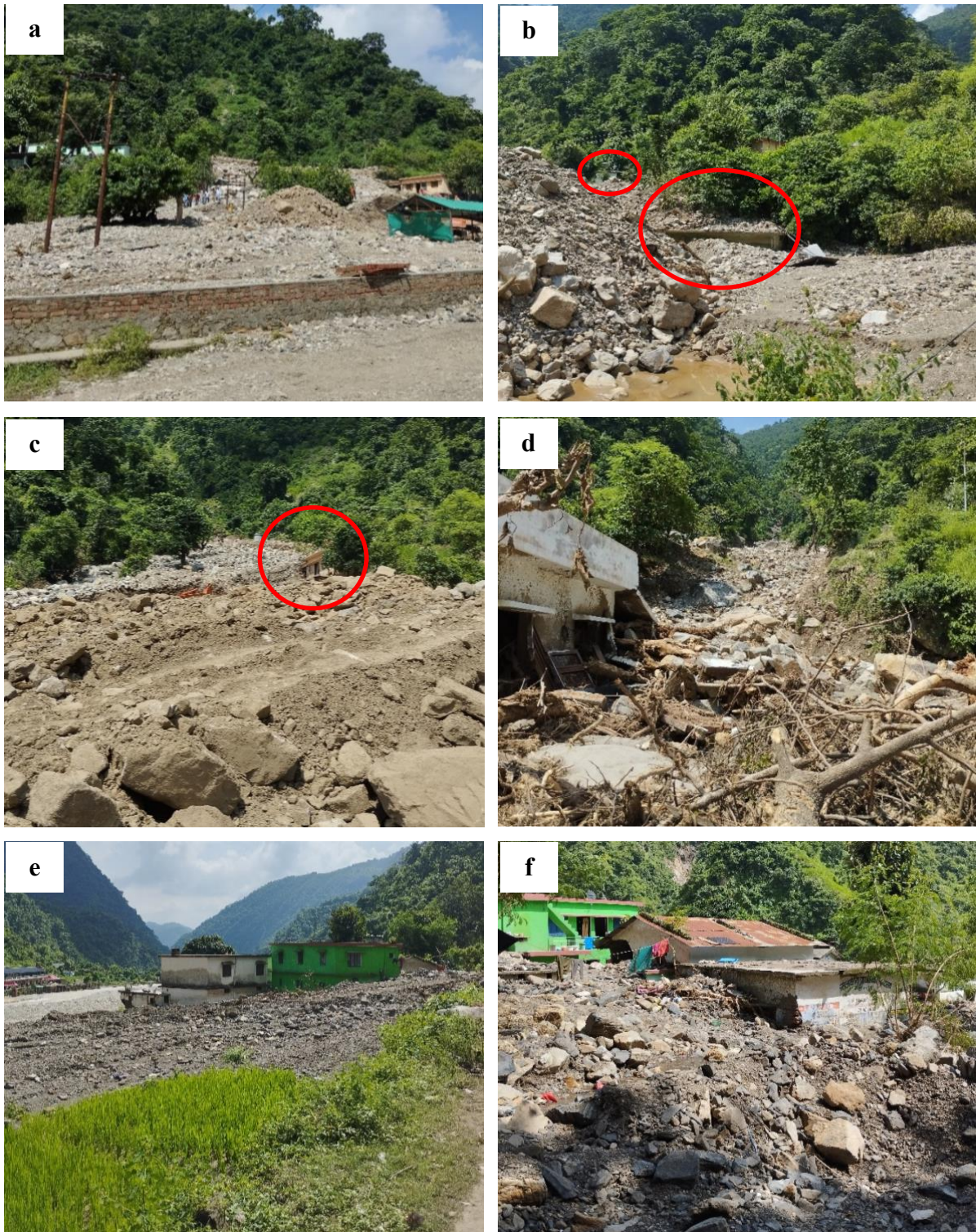


Figure 3. Photographs illustrate the devastated Bhaishwar and Sarkhet villages after heavy rainfall or cloudburst ensured debris flows; (a) accumulated debris in front of Musniwaa *Nallah* at Bhaishwar, (b) houses covered with debris at Bhaishwar, (c) Badly hit a house located at the course of Musniwala *Nallah* at Bhaishwar, (d) severely damaged a house due to change in course of Mushniwala *Nallah* at Bhaishwar, (e) overrun agriculture fields and damage to houses in front of the local stream at Sarkhet village, and (f) public and private properties covered with debris of local stream at Sarkhet village

Additionally, about 10-15m outside the left abutment of a motorable RCC bridge leading to Raipur- Thanu beyond Sports College near Raipur was destroyed by flood waters of Song River. Due to this, connectivity between the two areas was disrupted. Losses and damages including expected economic loss incurred in the affected region of Dehradun are given in Table 4.

4.3. Debris Flow and Flash Flood Incidences

According to eyewitnesses, high-intensity rainfalls coupled with thunderstorms caused debris flows through seasonal streams and flash floods in Bandal *Nadi*, causing considerable damage and destruction in the area. This is confirmed by the data of the automatic weather station of the Indian Meteorological Department (IMD) established in the Raipur area (38). Incident-wise details of damage incurred at various places along the Bandal *Nadi* and Song river are given in Table 4.

Table 4. Losses and damages including expected economic losses incurred in the affected region of Dehradun (Source: District Disaster Management Authority, Dehradun)

Sl. No.	Details of loss and damage	Expected economic loss (in lakhs)
1.	06 Tents at Four Banyan Resort in Maldeota	6.0
2.	25 houses damaged in Sarkhet	50.0
3.	Panchayat Ghar damaged in Sarkhet	10.0
4.	Primary School damaged in Sarkhet	12.0
5.	Damage to 6 Shops in Sarkhet	10.0
6.	Damage to 3.5 km electric line and about 20 electric poles along with 2 transformers in Maldeota to Sairki, Sarkhet and Saura Saroli	30.0
7.	A Bridge was damaged near Saura Saroli in Raipur area	200.0
8.	A Bridge damaged in Maldeota near Raipur	60.0
9.	Around 10-15 m part of the Bridge was destroyed beyond the sports college Raipur near in Song river	150.0
10.	a). 5 people killed while 3 persons injured along Musniwala <i>Nallah</i> due to cloudburst associated debris flows in Bhaishwar village b). damage to 01 house and 01 shops	12.0
11.	10 animals, 4 Calfs and 10 Goats died in Village Chhamroli/Sarkhet	5.20
12.	Around 8.25 ha of agricultural fields were damaged in Villages like Timli Man Singh, Sarkhet, Bhaishwar, Shairki, Chhamroli and Maldeota	200.00
13.	Damage to water lines in villages like Timli Man Sing, Sarkhet and Sairki	485.0

In the early hours (around 0215 hrs) of August 20, 2022, high-intensity rainfalls or cloudbursts-like events occurred in the upper reaches of Musniwala *Nallah*, causing high sediment laden discharge that generated sufficient momentum to devastate the Bhaishwar village, which is situated in front of its driveway. After water-saturated debris entered the village, bifurcating of *Nallah* into two channels. These materials flow down at high speed along moderate to gentle slopes through these channels resulting in massive damage to property and infrastructure. Many agricultural fields were destroyed while houses and shops were badly hit and some houses were covered with debris in this incidence (Figs. 4a to 4d). As many as 5 people died while 3 people injured in the same incidence.

Another debris flows through a seasonal stream took place at Sarkhet village following high-intensity rainfalls or cloudbursts in the morning hours (around 0215 hrs). This village is situated on the right bank of Bandal *Nadi* about 2km downstream of the Bhiswar village. It was observed that the village lies on the cone/fan material of a IInd order stream flows southeasterly direction and partly on the terrace material of the Bandal *Nadi*. A huge amount of water-saturated debris came down through this stream, causing widespread damage in the village. Connectivity of the region was disrupted and many houses were directly hit, while some were left under debris as well as agricultural fields overrun (Figs. 4e & 4f). Apart from this, the Panchayat Ghar along with Primary School also suffered heavy damage in this incidence.

Flash floods occurred through the Bandal *Nadi* following extremely heavy localised rainfall or cloudburst events. Unusually high sediment-laden discharge of the Bandal *Nadi* has eroded the terrace material on its both banks across the valley. Extensive property damages have occurred, particularly on the left bank of Dhantu Sera, east of Bauta on the right bank, at Kumalda on the left bank and just downstream of the confluence of Bandal *Nadi* and Song river on the right bank (Figs. 5a to 5d). The transport sector was also badly hit by flash food incidences, with about 500 m stretch of road between Dhantu Sera and Bhiswar villages and around 50m-100m stretch of road between Sarkhet and Bhiswar villages located on the right bank of Bandal *Nadi* were completely damaged (Figs 5e & 5f). Additionally, the road just downstream to the confluence of Bandal *Nadi* and Song river was also blocked, disrupting the connectivity in the devastated area.

5. Results and Discussion

High-intensity rainfalls in short periods or cloudburst events have resulted in the flow of water-saturated bouldery debris through local streams on which fan materials Bhiswar and Sarkhet villages are located, causing damage to several properties and killing 5 people while 12 families were rendered homeless. Similarly, Bastari village of Pithoragarh district (2016), Okhimath town of Rudraprayag district (2012), Jhakhla and Lah of Pithoragarh district (2009), Gadni and Musudiyar of Chamoli district (1993) were badly affected by cloudbursts ensured debris flows in the past wherein killing 148 people (17).

Geologically, the devastated area has folded belt and tectonically controlled valley, due to which the rocks of the area are highly fragile in nature. High-intensity rainfalls ensured flash flood and debris flow events, leading to rapid erosion of weak rocks and slope materials resulting in aggradation at various places along the Bandal *Nadi*. This caused changes in the course of Bandal *Nadi* at various places, particularly at Dhantu Sera, Bhiswar, Sarkhet, Kumalda and downstream areas wherein damage to agriculture fields, public transport, electricity, drinking water lines together with public and private properties. Earlier, Sangamchatti washed away and Gangori village was severely eroded in the Asi Ganga flash flood of 2012 (39) while the flash floods of June 2013 in the Mandakini river valley badly affected Kedarnath, Gaurikund, Chandrapuri, Augustmuni and Tilwara towns (17). In these incidences 35 and 4127 people were killed respectively.

From the geomorphological point of view, the habitation pattern of the devastated area is not found suitable, as most of the habitations are located near the stream and confluence areas in Quaternary deposits. Heavily concentrated rainfalls ensured debris flows and flash floods caused damage and destruction in these areas. As we all know that course of the stream keeps changing that surely hit its banks on which alluvium, colluvium and weak rocks exposure are placed. It is therefore recommended that houses should be constructed at a minimum distance

Cloudbursts Strike over Foothills Himalaya of Uttarakhand, India: A Case Study from Maldeota, Dehradun District

of 20-30m from small streams, whereas in the case of major streams, it should be 50-100m depending on site-specific conditions. In case of rock exposures distance may be less while in case of overburden material distance should be maximum from the stream/river.



Figure 4. Flash flood damages in both the banks of Bandal *Nadi*; (a) Damage to habitation of Dhantu Sera on the left bank, (b) damage to a building located East of Bouta at right bank, (c) Houses damaged at village Kumalda on the left bank, (d) damage to Four Banyans Spirit & Nature Resort downstream of the confluence of Bandal *Nadi* & Song *Nadi*, (e) washed away road on the right bank between Dhantu Sera and Bhaiwar villages, and (f) wiped out road between Sarkhet and Bhaiwar area on the right bank

The devastated area known as Maldeota, is one of the famous picnic spots of Dehradun city, which is visited by a large number of locals and outside people throughout the year. Due to increasing influx of tourists in the area, the hotel and shop facilities have been developed along the river banks. The concentration of economic opportunities near streams is largely responsible for increasing the risk of flash floods in the area. It has to be remembered that the stream is bound to reclaim its channel and both rise and fall of water level are processes which operate in all stream systems, hence any stream channel is vulnerable to encroachment in its regime. Therefore, it is recommended that any kind of construction activities in proximity of streams be prohibited in the area. Provisions of the Uttarakhand Flood Plain Zoning Act, 2012 should be invoked for doing so, in addition to those provided in Disaster Management Act, 2005.

The rehabilitation land is surrounded by a small stream in its North proximity which flows western direction in the area. Thickly bedded dolomitic limestone with intercalation of thin shale bands is observed in the proposed area, where the thickness of overburden including weathered rock is <1 m. The bedding planes were observed to dip in Northeasterly direction at angles varying from 40° to 50°. The joint sets were observed to dip at steep angles towards SE and SW (85°/170° and 60°/220°). Geologically, the proposed land was found to be feasible for rehabilitation purposes with proper due care of domestic waste-water as well as rainwater management.

6. Conclusions

High-intensity rainfalls ensured flash floods and debris flows caused considerable damage and destruction in the area. These caused death of 5 people and rendered 12 families homeless along with there was also damage to property and infrastructure. Bandal *Nadi* has changed its course and shifted towards the right and left banks by approximately 6 to 35 meters while Song river changed its course up to 50 meters due to flash floods. In this order, rehabilitation of those homeless families has been done as per Uttarakhand Rehabilitation Policy 2021. Besides, taking note of high damage in the devastated area, the author has made the following recommendations for managing the risk: (1) regulations of any kind of construction activities in proximity to stream/river, (2) prohibited construction in areas that were already affected in the flash flood and debris flow events, (3) reconstruction of the damaged stretch of road away from the river bed or elevated road from present high flood level, (4) avoiding excavation of river materials from river bed and *Nadi*/River training, especially where settlement poses risks, (5) implement structural measures in key zones, and (6) conducting disaster risk awareness campaigns among local residents and sharing indigenous knowledge about traditional habitation patterns with them.

As we all know that in recent times the incidents of cloudbursts have increased across the world due to climate change. The unpredictable nature of cloudburst is a cause of concern for planners and researchers. To address this issue, World Meteorological Organization (WMO) has developed the flash flood guidance system with global coverage (FFGS) which covers over 40% of the global population in more than 72 countries (40). This system aims to reduce the impacts of flash floods by enhancing early warning capabilities at regional and national levels. In this order, commissioning South Asia Flash Flood Guidance System for South Asian countries (India, Nepal, Bangladesh and Sri Lanka) on October 23, 2020 wherein India Meteorological Department is recognized as its regional Centre by WMO. In this context, preparations are being made to establish an early warning systems in the state of Uttarakhand as well. There is an urgent need for provision of early warning systems even at the local level, especially in areas identified with high risk of flash floods associated with high-intensity rains.

Acknowledgments

SK is grateful to Dr. Piyoosh Rautela, Executive Director, USDMA, Department of Disaster Management, Govt. of Uttarakhand for his guidance and encouragement to undertake these studies. Also thanks due to Mr. Harish Kainthola, Director, KainGeotech, Dehradun for his cooperation and support. This work is dedicated to those who were killed in this disaster.

Conflict of Interest

The author declares that he has no conflict of interest in this work.

Author Contributions

SK contributed to the design and implementation of the research, to the analysis of the results and to the writing of the manuscript.

References

- [1] Furtak, K., & Wolinska, A. (2023). The impact of extreme events as a consequence of climate change on the Soil moisture and on the quality of the soil environment and agriculture- A review. *Catena*, 231, 1-15.
- [2] Sati, V.P., & Kumar, S. (2022). Environmental and economic impact of cloudburst-triggered debris flows and flash floods in Uttarakhand Himalaya: a case study. *Geoenvironmental Disasters*, 9(5), 1-11.
- [3] Vijaykumar, P., Abhilash, S., Sreenath, A.V., Athira, U.N., Mohanakumar K., Mapes, B.E., Chakrapani, B., Sahai, A.K., Niyas, T.N., & Sreejith, O.P. (2021). Kerala floods in consecutive years - Its association with mesoscale cloudburst and structural changes in monsoon clouds over the west coast of India. *Weather and Climate Extremes*, 33, 1-14.
- [4] Wang, X.J., Zhang, J.Y., Shahid, S., Guan, E.H., Wu, Y.X., Gao, J., & He, R.M. (2014). Adaptation to climate change impacts on water demand. *Mitig. Adapt. Strat. G. L.* <https://doi.org/10.1007/s11027-014-9571-6>.
- [5] Li, Z., Gao, S., Chen, M., Gourley, J. J., Liu, C., Prein, A. F. & Hong, Y. (2022). The conterminous United States are projected to become more prone to flash floods in a high-end emissions scenario. *Communications earth and environment*, 86(3), 1-9.
- [6] Yang, Q., Liu, T., Zhai, J. & Wang, X. (2021). Numerical Investigation of a Flash flood process that occurred in Zhongdu river, Sichuan, China. *Frontiers in Earth Science*, 9, 1-11.
- [7] Ceribasi, G., & Ceyhunlu, A. I. (2021). Generation of 1D and 2D flood maps of Sakarya river passing through Geyve district of Sakarya city in Turkey. *Natural Hazards*, 105, 631-642.
- [8] Abdelkareem, M., & Mansour, A. M. (2023). Risk assessment and management of vulnerable areas to flash flood hazards in arid regions using remote sensing and GIS-based knowledge-driven techniques. *Natural Hazards*, 117(3), 2269-2295.

- [9] Umut, E. R. O. L., Kizmaz, Y., Özden, A., & Ceyhunlu, A. I. (2022). Evaluation of the Transportation Infrastructure Vulnerability in Kaynarca, Sakarya Basin from a Flood Spread Risk Perspective. *Academic Platform Journal of Natural Hazards and Disaster Management*, 3(1), 20-31.
- [10] Asthana, A.K.L., & Asthana, H. (2014). Geomorphic Control of Cloud Bursts and Flash floods in Himalaya with Special Reference to Kedarnath Area of Uttarakhand, India. *International Journal of Advancement in Earth and Environmental Sciences*, 2(1), 16- 24.
- [11] Khanduri, S. (2018). Landslide Distribution and Damages during 2013 Deluge: A Case Study of Chamoli District, Uttarakhand. *Journal of Geography and Natural Disaster*, 8(2), 1-10.
- [12] Khanduri, S., Sajwan, K.S., Rawat, A., Dhyani, C., & Kapoor S. (2018). Disaster in Rudraprayag District of Uttarakhand Himalaya: A Special Emphasis on Geomorphic Changes and Slope Instability. *Journal of Geography and Natural Disaster*, 8(1), 1-9.
- [13] Dikshit, A., Sarkar, R., Pradhan, B., Segoni, S., & Alamri, A. M. (2020). Rainfall induced landslides studies in Indian Himalayan region: A Critical review, *Applied Sciences*, 10, 2466, 1-24.
- [14] Kansal, M.L., & Singh, S. (2022). Flood Management Issues in hilly region of Uttarakhand (India) under changing climate conditions. *Water*, 14, 1879, 1-24.
- [15] Mandal, P., Prathigadapa, R., Srinivas, D., Saha, S., & Saha G. (2023). Evidence of structural segmentation of the Uttarakhand Himalaya and its implications for earthquake hazard. *Scientific reports*, 13, 2079, 1- 15.
- [16] Siddique, T., Haris, P. M., & Pradhan, S. P. (2022). Unraveling the geological and meteorological interplay during the 2021 Chamoli disaster, India. *Natural Hazards Research*, 2, 75–83.
- [17] Khanduri, S. (2020). Cloudbursts over Indian Sub-continent of Uttarakhand Himalaya: A Traditional Habitation Input from Bansoli, District- Chamoli, India. *International Journal of Earth Sciences Knowledge and Applications*, 2(2), 48-63.
- [18] Khanduri, S. (2022). Disastrous events of 2021 in Uttarakhand Province of India: Causes, Consequences and Suggestions for Disaster Risk Reduction (DRR). *International Journal of Earth Sciences Knowledge and Applications*, 4(2), 178-188.
- [19] Khanduri, S. (2022). Rain-induced Slope instability: Case study of Monsoon 2020 affected Villages in Pithoragarh District of Uttarakhand, India. *International Journal of Earth Sciences Knowledge and Applications*, 4(1), 1-18.
- [20] Khanduri, S. (2021). Formation and failure of natural dams in Uttarakhand Himalaya: An observation from Lwarkha, Chamba Tehsil of Tehri Garhwal district, India. *International Journal of Earth Sciences Knowledge and Applications*, 3(1), 12-22.
- [21] Khanduri, S. (2021). Flash flood struck Dhauliganga valley on February 7, 2021: A Case study of Chamoli district of Uttarakhand Himalaya in India. *Academic Platform Journal of Natural Hazards and Disaster Management*, 2(1), 1-15.

- [22] Khanduri, S., Saklani, R. D., & Chetry, B. M. (2023). Increasing risk of silent disaster in Uttarakhand Himalaya: An example from Higher Himalaya. *Journal of Disaster and Risk*, 6(3), 870-889.
- [23] Sundriyal, Y., Kumar, V., Chauhan, N., Kaushik, S., Ranjan, R., & Punia, M.K. (2023). Brief communication: The northwest Himalaya towns slipping towards potential disaster. *Natural Hazards and Earth System Science*, 23, 1425–1431.
- [24] Bahuguna, H., Kaistha, M. K., Singh, B., Das, S., Ahmad, T., & Rana, H. (2023). Preliminary Report on the Recent Event of Ground Subsidence at Joshimath, District Chamoli, Uttarakhand. *Geological Survey of India, Government of India*, 52.
- [25] Indian Standard (IS):1893, Part 1 (2002). Criteria for earthquake resistant design of structures, Bureau of Indian Standards, New Delhi.
- [26] Auden, J.B. (1934). The geology of the Krol belt. *Rec. Geol. Surv. India*, 67, 357-454.
- [27] Singh, A. K., Parkash B., Mohindra R., Thomas J. V., & Singvi, A. K. (2001). Quaternary alluvial fan sedimentation in the Dehradun Valley Piggyback Basin, NW-Himalaya, *Basin Research*, 13(4), 449-471.
- [28] Valdiya, K. S. (1980). *Geology of the Kumaun Lesser Himalaya*. Wadia Institute of Himalayan Geology, Dehra Dun, India. 249.
- [29] Thakur, V.C., Pandey, A.K., & Suresh, N. (2007). Late Quaternary–Holocene evolution of dun structure and the Himalayan Frontal fault zone of the Garhwal sub-Himalaya, NW India. *Journal of Asian Earth Sciences*, 29(2), 305-319.
- [30] Gansser, A. (1964). *Geology of the Himalayas*. Interscience Publications. Wiley, London, New York, 298.
- [31] Parkash, B., Sharma, R., & Roy, A. K. (1980). The Siwalik Group (Molasse) sedimentation shed by collision of continental plates. *Sedimentary Geology*, 25, 127-159.
- [32] Singh, A. K., Parkash B., Mohindra R., Thomas J. V., & Singhvi, A. K. (2001). Quaternary alluvial fan sedimentation in the Dehradun Valley Piggyback Basin, NW-Himalaya. *Basin Research*, 13(4), 449-471.
- [33] Nossin, J. J. (1971). Outline of the geomorphology of the Doon valley, northern U.P., India. *Z. Geomorph. N.F. Suppl. Bd. 12*. Berlin. Stuttgart, 18-50.
- [34] Nakata, T. (1972). Geomorphic history and crustal movement of the foothills of the Himalaya. Scientific report, Tohoku University Japan, 7th Series (Geography), 22, 39-177.
- [35] Rupke, N.A. (1975). Deposition of fine-grained sediments in the abyssal environment of the Algero-Balearic Basin, Western Mediterranean Sea. *Sedimentology* 22, 95–109.
- [36] Philip, G. (1995). Active tectonics in Doon valley. *Journal of Himalayan Geology*, 6, 55-61.

- [37] Pankaj, A. & Kumar, P. (2009). GIS-based Morphometric analysis of five major sub-waters of Song River, Dehradun District, Uttarakhand with Special reference to landslide incidences. *J. Indian Soc. Remote Sens.*, 37, 157-166.
- [38] Sain, K., Mehta, M., Kumar, V., Gupta, V. & Chauhan, P. (2023). A climate surprise-Slope instability triggered by heavy rain in Maldevta region, Dehradun, Uttarakhand, on 20 August, 2022. *Journal of Geological Society of India*, 99, 317-320.
- [39] Gupta V., Dobhal, D. P. & Vaideswaran, S. C. (2013). August 2012 cloudburst and subsequent flash flood in the Asi Ganga, a tributary of the Bhagirathi River, Garhwal Himalaya, India. *Current Science*, 105(2), 249-253.
- [40] <http://wmo.int/activities/flash-flood-guidance-system-global-coverage-ffgs>



© 2024 by the authors. Submitted for possible open access publication under the terms and conditions of the Creative Commons Attribution (CC BY) License (<http://creativecommons.org/licenses/by/4.0/>).